

Criterion for ultra-fast bubble walls: the impact of hydrodynamic obstruction

Wen-Yuan Ai,^{*1} Xander Nagels^{†2} and Miguel Vanvlasselaer^{‡2}

¹*Theoretical Particle Physics and Cosmology, King's College London,
Strand, London WC2R 2LS, UK*

²*Theoretische Natuurkunde and IIHE/ELEM, Vrije Universiteit Brussel, & The
International Solvay Institutes, Pleinlaan 2, B-1050 Brussels, Belgium*

Abstract

The Bodeker-Moore thermal friction [1] is usually used to determine whether or not a bubble wall can run away. However, the friction on the wall is not necessarily a monotonous function of the wall velocity and could have a maximum before it reaches the Bodeker-Moore limit. In this paper, we compare the maximal hydrodynamic obstruction, i.e., a frictional force in local thermal equilibrium that originates from inhomogeneous temperature distribution across the wall, and the Bodeker-Moore thermal friction. We study the former in a fully analytical way, clarifying its physical origin and providing a simple expression for its corresponding critical phase transition strength above which the driving force cannot be balanced out by the maximal hydrodynamic obstruction. We find that for large parameter space, the maximal hydrodynamic obstruction is larger than the Bodeker-Moore thermal friction, indicating that the conventional criterion for the runaway behavior of the bubble wall must be modified. We also explain how to apply efficiently the modified criterion to particle physics models and discuss possible limitations of the analysis carried out in this paper.

* wenyuan.ai@kcl.ac.uk

† xander.staf.a.nagels@vub.be

‡ miguel.vanvlasselaer@vub.be

Contents

1	Introduction	2
2	Bubble wall dynamics and the friction	4
3	Matching conditions for stationary and non-stationary walls	7
4	Maximal LTE pressure in the detonation regime	10
4.1	Bag model	10
4.2	$\mu\nu$ -model	12
5	Maximal hydrodynamic obstruction	13
6	Comparison with the Bodeker-Moore criterion	17
7	Comments on the validity of our approximations	20
8	Conclusion	21
A	Discussion on the departure from LTE	23

1 Introduction

Cosmological first-order phase transitions (FOPTs) have far-reaching phenomenological consequences. The collisions and mergers of the nucleated bubbles could result in a stochastic background of gravitational waves (GWs) [2–8].¹ The bubbles may also be pivotal for generating the cosmic matter-antimatter asymmetry [13–16]. Renewed interest in FOPTs in the early Universe has been triggered by the recent approval of the Laser Interferometer Space Antenna (LISA) project [17] and the detection of GWs [18]. Besides LISA, many other space-based GW detectors have been proposed, such as Big Bang Observer (BBO) [19], Deci-hertz Interferometer Gravitational wave Observatory (DECIGO) [20], Taiji [21], and TianQin [22].

FOPTs may also be relevant for producing primordial black holes [23–34], particle dark matter [35–37], and intergalactic magnetic fields [38, 39]. All the above-mentioned processes depend crucially on the regime of the bubble wall expansion, making the terminal velocity ξ_w a key parameter. In recent years, ultrarelativistic bubble walls (bubbles expanding with a Lorentz factor $\gamma_w \equiv 1/\sqrt{1 - \xi_w^2} \gg 1$) have been used for phenomenological studies on baryogenesis [40–44] and dark matter production [45–47]. For the application of ultrarelativistic bubble walls, it is extremely important to determine whether the bubble wall can enter into the ultrarelativistic regime or not. Furthermore, runaway and non-runaway walls could have very different GW signals (see Refs. [7, 8, 48–50] for reviews and see, e.g., Refs. [51, 52] for studies on supercooled PTs).

Estimates of the terminal wall velocity are usually based on kinetic theory [53–56], improvement of it [40, 57, 58], or holographic methods for strongly coupled theories [59–63]

¹Excitingly, such an SGWB has been reported by several Pulsar Timing Array projects [9–12] recently, whose source however may prefer a supermassive black hole explanation.

(see Ref. [64] for a quasiparticle (quasiglons) method). Typically, calculating the terminal wall velocity is a very challenging task, and has only been performed for a limited number of models [54–56, 58, 65, 66]. In such computations, one needs to solve the scalar field equation of motion (EoM) coupled to the Boltzmann equations describing the particles in the plasma. Simplifications can be obtained by assuming local thermal equilibrium (LTE) [67–74] or in the ultrarelativistic regime [1, 75–80]. In LTE, the wall velocity can be determined with the help of an additional matching condition for the hydrodynamic quantities on both sides of the wall [70, 72]. The LTE approximation is shown to work well for strongly coupled theories [74] whose FOPT-related phenomenology has been studied in, e.g., Refs. [61, 81–93].

In the case of the ultrarelativistic regime, one may use the ballistic approximation [53, 56]. Mathematically, the ballistic approximation amounts to

$$L_w \ll \gamma_w L_{\text{MFP}} \quad (\text{ballistic condition}), \quad (1)$$

where L_w is the width of the wall in the wall frame, L_{MFP} is the mean free path of the incoming particles in the plasma frame. In this case, the particles do not (have time to) collide with each other when they pass through the wall. The pressure on the bubble wall is simply due to the transmission of the particles from the outside to the inside, and their reflection from the wall. It is a *monotonically increasing* function of the velocity. This pressure, at large $\gamma_w \gg 1$, asymptotes to [1]

$$\mathcal{P}_{\text{BM}} \simeq \sum_i g_i c_i \frac{\Delta m_i^2 T_n^2}{24}, \quad (2)$$

where $c_i = 1(1/2)$ for bosons (fermions), g_i is the number of internal degrees of freedom, T_n is the nucleation temperature, and Δm_i is the mass gain of the particle as it transits from the exterior to the interior of the bubble. The criterion

$$\mathcal{P}_{\text{driving}} > \mathcal{P}_{\text{BM}} \quad (\text{Bodeker and Moore (BM) criterion}), \quad (3)$$

where $\mathcal{P}_{\text{driving}}$ is the driving pressure, is frequently used to determine whether a wall runs away or not. Note that \mathcal{P}_{BM} in Eq. (2) is only the friction in the ultrarelativistic regime at the leading order in γ_w . Other particle-number-changing processes typically induce additional friction that depends on γ_w [75, 76, 78, 79]. There can also be additional friction due to heavy new physics [77] that is also independent of γ_w . In this paper, we will not consider those types of contributions. Therefore, one needs to assume that there is no additional γ_w -independent friction in the ultrarelativistic regime other than the BM thermal friction. And we interpret “runaway” in this paper as that the wall can enter into a regime with extremely large γ_w for which other γ_w -dependent (if present) pressures become comparable with \mathcal{P}_{BM} .

However, the total friction on the wall does not need to be a monotonous function of the wall velocity and could have a maximum before it reaches the Bodeker-Moore limit. Indeed, it is observed in Refs. [57, 58, 72] that there is a pressure barrier peaked at the Jouguet velocity ξ_J . This peak is largely due to the hydrodynamic obstruction [67], a frictional force originating from inhomogeneous temperature distribution across the wall in LTE, as shown in Ref. [58].² The hydrodynamic obstruction will also be called the LTE force occasionally.

In this paper, we compare the maximal hydrodynamic obstruction with the Bodeker-Moore (BM) thermal friction Eq (2). We show that the former can be larger than the latter

²Ref. [94] argues that out-of-equilibrium effects should be comparable to the hydrodynamic obstruction, based on the so-called extended fluid Ansatz [95, 96].

in large regions of the parameter space and hence the runaway criterion must be reconsidered. This means that in many models while the BM thermal friction cannot stop the wall's acceleration, the hydrodynamic obstruction can however do this job. We work out the critical phase transition strengths, $\alpha_{n,\text{crit}}^{\text{BM/LTE}}$, above which the driving force cannot be balanced out by the maximal hydrodynamic obstruction/the BM thermal friction, and compare them with each other. Defining the ratio of the number of degrees of freedom (DoFs) in the broken and symmetric phases, $b \equiv a_-/a_+$, we find that hydrodynamic obstruction becomes more relevant than the BM thermal friction in prohibiting runaway for $b \lesssim 0.85$. Although the value of b in the standard model (SM) at the electroweak phase transition (EWPT) is close to one, $b_{\text{EWPT}} \sim 0.9$, many beyond-standard-model (BSM) phase transitions feature a much smaller b , like in minimal toy models of phase transition with two scalar fields [97], minimal models of $B - L$ breaking [44, 98], Peccei-Quinn symmetry breaking [99], or conformal symmetry breaking [98, 100]. Deconfinement-confinement phase transitions like in the composite Higgs also feature a large change in the number of DoFs [74, 101–103].

The maximal hydrodynamic obstruction has been partly studied in Ref. [72]. There, however, no attention has been paid to the comparison with the BM thermal friction. Furthermore, we give a simpler derivation of the critical phase transition strength $\alpha_{n,\text{crit}}^{\text{LTE}}$ without solving the fluid equations. Therefore, our derivation can be very easily implemented in, e.g., Mathematica. We also provide a fit for the obtained $\alpha_{n,\text{crit}}^{\text{LTE}}(b)$ as a function of b .

The paper is organized as follows. In the next section, we derive the general formulae for the driving and frictional pressures for general wall motions (not necessarily stationary) from the EoM of the scalar field. In Sec. 3, we derive a different formula for the frictional pressure based on the matching conditions. In Sec. 4, we study the maximal LTE friction *in the detonation regime* which however is *not* the maximal hydrodynamic obstruction. The latter occurs in the hybrid regime and is studied in Sec. 5. In Sec. 6, we compare the maximal hydrodynamic obstruction with the BM thermal friction. In Sec. 7, we comment on the validity of the approximations used in this work and give some caveats. We conclude in Sec. 8. In the Appendix, we also briefly discuss how to include the out-of-equilibrium effects in the analysis.

2 Bubble wall dynamics and the friction

Analysis of the friction on bubble walls is usually based on the following EoM for the background field [55, 56],

$$\square\phi + \frac{dV(\phi)}{d\phi} + \sum_i \frac{dm_i^2(\phi)}{d\phi} \int \frac{d^3\mathbf{p}}{(2\pi)^3 2E_i} f_i(p, z) = 0, \quad (4)$$

where $\square = \partial_\mu \partial^\mu$, $f_i(p, z)$ are the particle distribution functions, and $E_i = \sqrt{\mathbf{p}_i^2 + m_i^2}$ the particle energies. We shall assume a planar wall expanding in the z direction.

For a bubble wall with a constant velocity, which we will refer to as a *stationary* wall, one can always work in the wall rest frame where all quantities are time independent. However, for a general motion, we cannot define a global rest frame of the wall. But we can still define an “instantaneous” wall rest frame which can help us find the expressions for the driving and frictional pressures. With fixed x and y , the worldline of the wall can be parameterized by a proper time τ . Near an arbitrarily chosen proper time of the wall, we define an instantaneous comoving rest frame as follows. First, we assume a certain Ansatz for the wall in the plasma frame from which the wall velocity and acceleration can

be read [104]. For example, one can take

$$\phi(t', z') = \frac{v_b}{2} [\tanh[(z' - z'_0(t'))/L'_w] + 1], \quad (5)$$

where $\{t', z'\}$ are the coordinates in the plasma frame and L'_w is the wall width observed in that frame. The function $z'_0(t')$ describes the trajectory of the wall. We can choose $t' = 0$ at the reference point of the worldline (corresponding to the chosen τ). Then $z'_0(t) = z'_0 + v_w t' + \frac{1}{2} a t'^2 + \mathcal{O}(t'^3)$. The velocity v_w is used to define the (instantaneous) comoving coordinates

$$z = \gamma_w(z' - z'_0 - v_w t'), \quad t = \gamma_w[t' - v_w(z' - z'_0)]. \quad (6)$$

In the instantaneous rest frame of the wall, one can choose $z = 0$ as the position of the wall and at the origin of coordinates $t = 0$. It is easy to show that the first time derivative of ϕ in the instantaneous comoving frame, $\partial_t \phi(0) \equiv \dot{\phi}(0)$, is vanishing. The second time derivative of ϕ , $\ddot{\phi}(0)$, depends on the acceleration a and vanishes also if $a = 0$ which corresponds to a stationary wall.

In the instantaneous comoving frame, multiplying the EoM by $\partial_z \phi$ and integrating over z , one gets

$$\int_{-\delta}^{\delta} dz (\partial_z \phi) \left(\ddot{\phi}(0)|_{\tau} - \partial_z^2 \phi + \frac{dV(\phi)}{d\phi} + \sum_i \frac{dm_i^2(\phi)}{d\phi} \int \frac{d^3 \mathbf{p}}{(2\pi)^3 2E_i} f_i(p, z) \right) = 0, \quad (7)$$

where δ is a length much larger than the wall width, and effectively can be taken to be infinity in the present context. Above, we also have Taylor expanded quantities in t at $t = 0$ and kept the leading contributions. The second term is vanishing because the integrand $(\partial_z \phi) \partial_z^2 \phi$ is a total derivative and $\partial_z \phi$ vanishes for large $|z|$ (for any τ). The term with $\dot{\phi}(0)|_{\tau}$ is related to the acceleration of the wall at τ as discussed above. Thus we obtain

$$- \int_{-\delta}^{\delta} dz (\partial_z \phi) \ddot{\phi}(0)|_{\tau} = \mathcal{P}_{\text{driving}} - \mathcal{P}_{\text{friction}}, \quad (8)$$

where

$$\mathcal{P}_{\text{driving}} = \int_{-\delta}^{\delta} dz (\partial_z \phi) \frac{dV(\phi)}{d\phi} = \int_{-\delta}^{\delta} dz \frac{dV(\phi(z))}{dz}, \quad (9)$$

$(\frac{dV(\phi(z))}{dz}) > 0$ since the zero-temperature potential outside of the wall is higher than that inside the wall, see Fig. 1), and

$$\mathcal{P}_{\text{friction}} = - \int_{-\delta}^{\delta} dz (\partial_z \phi) \left(\sum_i \frac{dm_i^2(\phi)}{d\phi} \int \frac{d^3 \mathbf{p}}{(2\pi)^3 2E_i} f_i(p, z) \right). \quad (10)$$

The sum in the last expression is to be taken on the species changing mass across the wall. Although the above expressions implicitly depend on τ , we expect that their dependence on τ from the τ -dependence in ϕ disappears or becomes very weak as long as δ is much larger than the wall width. Thus $\mathcal{P}_{\text{driving}}$ can be identified as the zero-temperature potential difference between the symmetric and broken phases,

$$\mathcal{P}_{\text{driving}} = \Delta V, \quad (11)$$

and is therefore not a function of the temperature nor τ . $\mathcal{P}_{\text{friction}}$ can still be τ -dependent due to the time-dependence in the distribution functions which should be determined by solving the Boltzmann equation. A stationary motion is reached when $\mathcal{P}_{\text{driving}} = \mathcal{P}_{\text{friction}}$, which leads to $\ddot{\phi}(0)|_{\tau} = 0$, as expected. Looking at Eq. (10), it would seem that $\mathcal{P}_{\text{friction}}$ only depends on bath particles directly coupling with the scalar field ϕ with a wall-dependent mass (particles that we will call *active particles* in what follows). This is not exactly the case, because the distribution functions depend on the interactions among all the particles in the bath. Writing $f_i = f_i^{\text{eq}} + \delta f_i$, the frictional pressure can be further decomposed into two parts

$$\mathcal{P}_{\text{friction}} = \mathcal{P}_{\text{LTE}} + \mathcal{P}_{\text{dissipative}}, \quad (12)$$

where $\mathcal{P}_{\text{dissipative}}$ is given by Eq. (10) with f_i replaced by the out-of-equilibrium part δf_i . In this paper, we are interested in \mathcal{P}_{LTE} which reads

$$\begin{aligned} \mathcal{P}_{\text{LTE}} &= - \int_{-\delta}^{\delta} dz (\partial_z \phi) \left(\sum_i \frac{dm_i^2(\phi)}{d\phi} \int \frac{d^3\mathbf{p}}{(2\pi)^3 2E_i} f_i^{\text{eq}}(p, z; T) \right) \\ &= - \int_{-\delta}^{\delta} dz (\partial_z \phi) \frac{\partial V_T(\phi, T)}{\partial \phi}. \end{aligned} \quad (13)$$

Here $V_T(\phi, T)$ is the finite-temperature corrections to the potential in the non-interacting-gas approximation [105] and T , which in general depends on z , is the temperature of all the particles being in local thermal equilibrium. Remembering the z -dependence in $V_T(\phi(z), T(z))$ and using the chain rule for derivatives, \mathcal{P}_{LTE} can be further written as

$$\mathcal{P}_{\text{LTE}} = -\Delta V_T + \int_{-\delta}^{\delta} dz \frac{\partial V_T}{\partial T} \frac{\partial T}{\partial z}. \quad (14)$$

Note that there is no clear criterion to distinguish between the driving and friction forces. Different authors may attribute the same force to either the driving force or the friction force. Our definitions above are different from those used in Ref. [70] where ΔV_T was identified as a part of the driving force. However, the quantity $\mathcal{P}_{\text{friction}} - \mathcal{P}_{\text{driving}}$ is invariant under different identifications. A merit of the definitions we are using is that the driving pressure is constant, in agreement with the convention used in Refs. [1, 75].

In this paper, we shall assume LTE for the plasma and study $(\mathcal{P}_{\text{friction}} - \mathcal{P}_{\text{driving}})(\xi_w)$ as a function of the wall velocity. In particular, we are interested in its maximum, $(\mathcal{P}_{\text{LTE}} - \mathcal{P}_{\text{driving}})_{\text{max}} \equiv (\mathcal{P}_{\text{friction}} - \mathcal{P}_{\text{driving}})_{\xi_w = \xi_{\text{peak}}}$ (see the left panel of Fig. 2 below). If $(\mathcal{P}_{\text{LTE}} - \mathcal{P}_{\text{driving}})_{\text{max}} > 0$, then there should be a stationary solution for the wall in LTE. On the other hand, if $(\mathcal{P}_{\text{LTE}} - \mathcal{P}_{\text{driving}})_{\text{max}} < 0$, a stationary solution is not possible and the wall runs away unless $\mathcal{P}_{\text{dissipative}}$ becomes large enough to stop the acceleration of the wall. Since $\mathcal{P}_{\text{driving}}$ is constant, $(\mathcal{P}_{\text{LTE}} - \mathcal{P}_{\text{driving}})_{\text{max}}$ corresponds to $\mathcal{P}_{\text{LTE}}^{\text{max}}$, the maximal LTE frictional pressure.

In realistic situations, the plasma is typically out of equilibrium. However, if we assume that out-of-equilibrium effects would add more friction to the wall, which is confirmed in a simple model in Ref. [58] and also in the Appendix for general case, $\mathcal{P}_{\text{LTE}}^{\text{max}} > \mathcal{P}_{\text{driving}}$ implies $\mathcal{P}_{\text{friction}}^{\text{max}} > \mathcal{P}_{\text{driving}}$ and the former can serve as a conservative condition for non-runaway bubble walls.

It is still not clear how to compute \mathcal{P}_{LTE} using the formula (14) directly. In the next section, we derive another form of \mathcal{P}_{LTE} that can be conveniently used to determine $\mathcal{P}_{\text{LTE}}^{\text{max}}$.

3 Matching conditions for stationary and non-stationary walls

The hydrodynamics of the bubble growth is based on the total energy-momentum conservation. Usually, a stationary wall is assumed and one works in the rest frame of the wall. Here again, we do not assume a stationary motion of the wall. The energy-momentum tensors for the scalar background and the fluid read

$$T_{\phi}^{\mu\nu} = (\partial^{\mu}\phi)\partial^{\nu}\phi - g^{\mu\nu} \left(\frac{1}{2}(\partial\phi)^2 - V(\phi) \right), \quad (15)$$

$$T_f^{\mu\nu} = (e + p)u^{\mu}u^{\nu} - g^{\mu\nu}[p + V(\phi)], \quad (16)$$

where e and p are the energy density and pressure with zero-temperature contributions included, u^{μ} is the fluid four-velocity. The matching conditions are obtained from the $\nu = 0$ and $\nu = 3$ components of $\nabla_{\mu}T^{\mu\nu} = 0$. Working in the instantaneous comoving frame and writing $u^{\mu} = \gamma(z)(1, 0, 0, -v(z))$, one obtains

$$\partial_z(\omega\gamma^2v) = 0, \quad (17a)$$

$$- (\partial_z\phi)\ddot{\phi}(0)|_{\tau} + \partial_z \left[\omega\gamma^2v^2 + \frac{1}{2}(\partial_z\phi)^2 + p \right] = 0, \quad (17b)$$

where $\omega \equiv (e + p)$ is the enthalpy. Above, we have assumed that all the first derivatives in time of the hydrodynamic quantities are vanishing.³ Integrating over z , one obtains

$$\omega_+\gamma_+^2v_+ = \omega_-\gamma_-^2v_-, \quad (18a)$$

$$\begin{aligned} - \int_{-\delta}^{\delta} dz (\partial_z\phi)\ddot{\phi}(0)|_{\tau} &= [\omega_-\gamma_-^2v_-^2 + p_-] - [\omega_+\gamma_+^2v_+^2 + p_+] \\ &\equiv \Delta V - \Delta(-V_T + \omega\gamma^2v^2), \end{aligned} \quad (18b)$$

where a subscript “ \pm ” denotes quantities in front of/behind the bubble wall. To be explicit, $\omega_+ = \omega_s(T_+)$, $\omega_- = \omega_b(T_-)$ (and similarly for p_{\pm}), where the label “ s/b ” denotes the symmetric/broken phase, see Fig. 1. In the last equality of Eq. (18b) we have used the thermodynamic relation in LTE $p = -V_{\text{eff}}(\phi) \equiv -V(\phi) - V_T(\phi)$, and so it is valid only for LTE [70]. Comparing Eq. (18b) with Eqs. (8) and (11), we thus obtain

$$\mathcal{P}_{\text{LTE}} = -\Delta V_T + \bar{\mathcal{P}}_{\text{LTE}}, \quad (19)$$

where

$$\bar{\mathcal{P}}_{\text{LTE}} \equiv \Delta\{\omega\gamma^2v^2\} = \Delta\{(\gamma^2 - 1)Ts\} \quad (20)$$

with $s = \omega/T$ being the entropy density. Using Eq. (18a), one can rewrite it as

$$\bar{\mathcal{P}}_{\text{LTE}} = \omega_+\gamma_+^2v_+(v_+ - v_-). \quad (21)$$

³Whether this assumption is true or not cannot be solely determined by the total energy-momentum conservation. It depends on the microscopic details of how the scalar field interacts with the plasma. If this assumption is not true, one would have additional terms in Eqs. (17) expressed by the first derivatives in time of the hydrodynamic quantities. But since for $\ddot{\phi}(0)|_{\tau} = 0$ (i.e. vanishing acceleration of the wall) the time dependence disappears in all quantities in the comoving frame, the first time derivatives of the hydrodynamic quantities in the instantaneous comoving frame must depend on the acceleration of the wall a and vanish as $a \rightarrow 0$. Since the critical phase transition strength $\alpha_{n,\text{crit}}^{\text{LTE}}$ is given ultimately by a stationary motion ($a = 0$, see below), our derivation of it would not be changed even if the present assumption is not fully true.

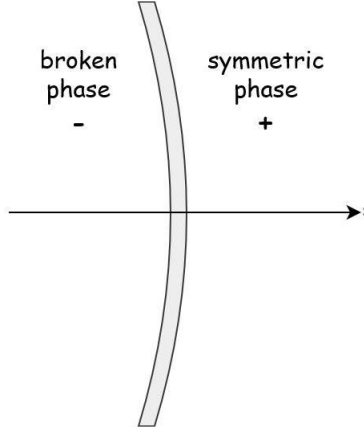


Figure 1: Rest frame of the bubble wall used for the matching conditions.

In LTE, there is an additional matching condition due to the entropy conservation [70]⁴

$$\partial_\mu(su^\mu) = 0 \quad \Rightarrow \quad s_+\gamma_+v_+ = s_-\gamma_-v_-. \quad (22)$$

The above condition is a special situation of the non-negativity of entropy production [106]. Using Eq. (18a), it can be also written as

$$\frac{T_+}{T_-} = \frac{\gamma_-}{\gamma_+}. \quad (23)$$

In Appendix A, we explain how to extend this picture if there is a large entropy injection and we argue that the LTE limit provides a *lower bound* on the resistance to the bubble expansion.

If we impose $\ddot{\phi}(0)|_\tau = 0$, i.e., vanishing acceleration, we arrive at three matching conditions for three unknown hydrodynamic quantities $\{T_-, v_+, v_-\}$ (T_+ can be related to the nucleation temperature T_n which is a given parameter characterizing the phase transition), i.e. Eqs. (18) (with $\ddot{\phi}(0)|_\tau = 0$) and Eq. (23). We therefore can fully determine all these three quantities, and thus also the wall velocity ξ_w (e.g., for detonations, $\xi_w = v_+$). To study the frictional force in LTE as a function of ξ_w , $\ddot{\phi}(0)$ must be allowed to take any value so that the wall velocity ξ_w becomes a variable. In this case, one should in principle only use the matching conditions (18a), (23) and the definition of \mathcal{P}_{LTE} given in Eqs (19), (20). However, as we will see shortly, for the derivation of the critical phase transition strength $\alpha_{n,\text{crit}}^{\text{LTE}}$, $\ddot{\phi}(0)|_\tau = 0$ can be imposed.

It is argued in Ref. [72], based on numerical results and previous works [57, 58], that the hydrodynamic obstruction is maximal when the wall velocity ξ_w is very close to the Jouguet velocity ξ_J . We will elaborate on this point in Sec. 5. We can however already anticipate the important points: the hydrodynamic obstruction originates mainly from the heating due to the shock wave existing in front of the bubble, which decreases the effective phase transition strength felt by the bubble wall. This heating becomes more efficient as the velocity of the shock-wave front increases ξ_{sw} (see Eq. (62a) and the heating parameter Eq. (63)). The velocity of the shock-wave front has however to be smaller than the Jouguet velocity $\xi_{\text{sw}} \leq \xi_J$, which implies that the maximal heating, and thus obstruction, will occur at the Jouguet velocity. For larger wall velocities, the LTE pressure decreases (when the

⁴The derivation of this condition involves only first derivatives in time and hence should be valid in the instantaneous comoving frame for non-stationary walls.

motion becomes a detonation), because the shock wave disappears, and thus the heating vanishes.

The typical behavior of the total pressure on the wall in LTE is shown in the left panel of Fig. 2. Since the Jouguet velocity is a connecting point between the hybrid and detonation regimes, one might think that $\mathcal{P}_{\text{LTE,hyb}}^{\text{max}} = \mathcal{P}_{\text{LTE,det}}^{\text{max}}$. However, this is generically not true as indicated by the very steep slope at ξ_J . The reason behind this is the sudden disappearance of the shock wave when one moves from the hybrid regime to the detonation regime which typically leads to a lower $\mathcal{P}_{\text{LTE,det}}^{\text{max}}$ compared with $\mathcal{P}_{\text{LTE,hyb}}^{\text{max}}$. Only when the ratio of the enthalpies in the broken and symmetric phases is very close to one, is the equality $\mathcal{P}_{\text{LTE,hyb}}^{\text{max}} = \mathcal{P}_{\text{LTE,det}}^{\text{max}}$ satisfied [72], see Sec. 5 for more details. Therefore, we have

$$\mathcal{P}_{\text{LTE}}^{\text{max}} = \mathcal{P}_{\text{LTE,hyb}}^{\text{max}} \geq \mathcal{P}_{\text{LTE,det}}^{\text{max}}. \quad (24)$$

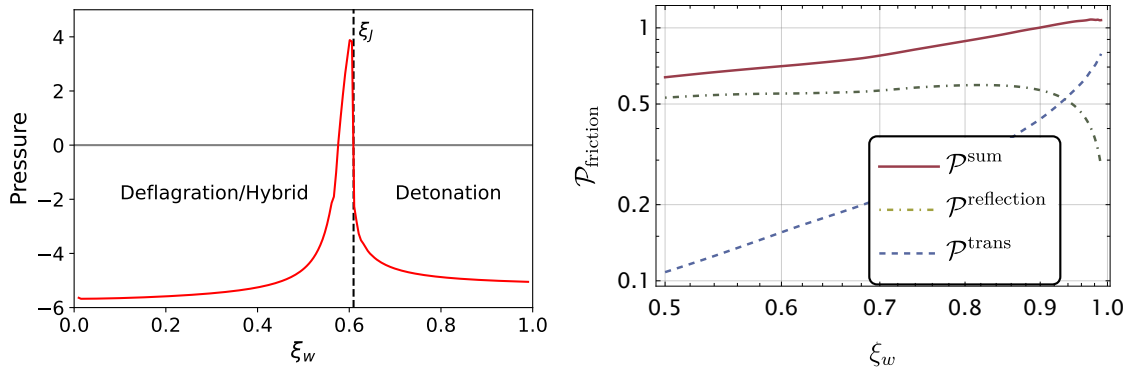


Figure 2: Left: Example of $\mathcal{P}_{\text{LTE}} - \mathcal{P}_{\text{driving}}$ (in arbitrary units) as a function of the wall velocity ξ_w for a given phase transition strength α_n , based on results of Ref. [58]. $\mathcal{P}_{\text{LTE}}^{\text{max}}$ occurs slightly before the Jouguet velocity ξ_J . Plot taken from Ref. [72]. Right: Example of the total frictional pressure due to transmission and reflection in the ballistic picture that are assumed to become more and more exact for a larger and larger γ_w . It is a monotonically increasing function and saturates at the BM value.

As α_n increases, one should expect that the peak of the red curve in the left panel of Fig. 2 would move down due to the increase of $\mathcal{P}_{\text{driving}}$. At a critical value, denoted as $\alpha_{n,\text{crit}}^{\text{LTE}}$, the peak would touch exactly the zero line. For bigger α_n , $\mathcal{P}_{\text{LTE}} - \mathcal{P}_{\text{driving}}$ cannot equal zero for all $\xi_w \in [0, 1)$ and thus the bubble wall runs away assuming LTE. Therefore, this value $\alpha_{n,\text{crit}}^{\text{LTE}}$ provides a criterion for runaway walls in LTE;

$$\text{LTE runaway criterion : } \alpha_n > \alpha_{n,\text{crit}}^{\text{LTE}}. \quad (25)$$

Note that the peak has a narrow width, which means that when $\alpha_n < \alpha_{n,\text{crit}}^{\text{LTE}}$, the wall velocity is typically close to ξ_J such that $\xi_w \approx \xi_J$ may be a good approximation when the stationary motion is caused by hydrodynamic obstruction [58]. Since the peak decreases dramatically after ξ_J , only deflagration/hybrid (or ultrarelativistic detonation) solutions are viable [72]. This may also be true if out-of-equilibrium effects are included [58] (see, however, Ref. [107]).

Similarly, there is also the runaway criterion based on the Bodeker-Moore leading-order friction on ultrarelativistic bubble walls [1];

$$\text{Bodeker-Moore runaway criterion : } \alpha_n > \alpha_{n,\text{crit}}^{\text{BM}}. \quad (26)$$

In the right panel of Fig. 2, we show the frictional pressures in the ballistic approximation, obtained by computing the momentum exchange between the wall and particles that transmit from the outside to the inside of the wall $\mathcal{P}^{\text{trans}}$, and that bounce off from the wall $\mathcal{P}^{\text{reflection}}$. In this type of calculation, the plasma outside of the wall is assumed to be unperturbed, and thus the calculation is typically valid for a relativistic detonation regime. The total frictional pressure \mathcal{P}^{sum} approaches the BM limit for $\gamma_w \gg 1$ where $\mathcal{P}^{\text{reflection}}$ approaches zero. It is expected that the red curve in the left panel of Fig. 2 is followed by the dark red curve (when $-\mathcal{P}^{\text{driving}}$ is included) from the right panel when the same particle physics model is considered.

Since $\alpha_{n,\text{crit}}^{\text{LTE}}$ and $\alpha_{n,\text{crit}}^{\text{BM}}$ are not necessarily equal to each other, we propose a modified runaway criterion in this work;

$$\text{Modified runaway criterion : } \alpha_n > \max\{\alpha_{n,\text{crit}}^{\text{LTE}}, \alpha_{n,\text{crit}}^{\text{BM}}\}. \quad (27)$$

Below, we shall derive both $\alpha_{n,\text{crit}}^{\text{LTE}}$ and $\alpha_{n,\text{crit}}^{\text{BM}}$, and compare them. As we shall see, $\alpha_{n,\text{crit}}^{\text{LTE}}$ can be larger than $\alpha_{n,\text{crit}}^{\text{BM}}$ in a large parameter space, indicating that the peak of the LTE force is larger than the Bodeker-Moore thermal friction. For, $\alpha_n \in (\alpha_{n,\text{crit}}^{\text{BM}}, \alpha_{n,\text{crit}}^{\text{LTE}}]$, the wall acceleration would be stopped by the LTE force even though it cannot be stopped by the BM thermal friction that exists in the ultrarelativistic regime.

Since $\alpha_{n,\text{crit}}^{\text{LTE}}$ is given by $\mathcal{P}_{\text{LTE}}^{\text{max}} = \mathcal{P}^{\text{driving}}$, i.e., when the peak touches the zero line of Fig. 2 (left panel), we actually can use the additional matching condition (that is valid only for stationary walls)

$$\omega_- \gamma_-^2 v_-^2 + p_- = \omega_+ \gamma_+^2 v_+^2 + p_+, \quad (28)$$

in deriving $\alpha_{n,\text{crit}}^{\text{LTE}}$. With the conditions (18a) and (28), one has [70]

$$v_- = \frac{1}{6v_+} \left[1 - 3\alpha_+ + 3(1 + \alpha_+) v_+^2 \pm \sqrt{(1 - 3\alpha_+ + 3(1 + \alpha_+) v_+^2)^2 - 12v_+^2} \right], \quad (29)$$

where

$$\alpha_+ \equiv \frac{\Delta\theta}{3\omega_+}, \quad \text{with} \quad \theta = \rho - 3p, \quad (30)$$

and $+$ and $-$ sectors correspond to deflagration/hybrid and detonation regimes, respectively. One can then substitute Eq. (29) into Eq. (21).

4 Maximal LTE pressure in the detonation regime

Before we discuss the maximal hydrodynamic obstruction in LTE, equivalently, $\alpha_{n,\text{crit}}^{\text{LTE}}$, we first discuss the maximal LTE pressure in the *detonation* regime, $\alpha_{n,\text{max}}^{\text{det}}$. This simpler analysis serves as a warm-up for the more complicated analysis given in the next section. Below, we carry out our analysis for the bag equation of state (EoS) and one of its generalizations where the sound speed can deviate from $1/\sqrt{3}$.

4.1 Bag model

To close the system of equations, we now need to introduce an EoS. We first consider the *Bag model* for which we have

$$e_s(T) = a_+ T^4 + \epsilon, \quad p_s(T) = \frac{1}{3} a_+ T^4 - \epsilon, \quad (31)$$

$$e_b(T) = a_- T^4, \quad p_b(T) = \frac{1}{3} a_- T^4, \quad (32)$$

where a_{\pm} and ϵ are constants and we used the convention $\epsilon \equiv \Delta V$. With this EoS, $\alpha_+ = \epsilon/(a_+ T_+^4)$.

In the detonation regime, $v_+ = \xi_w$, $T_+ = T_n$, $\alpha_+ = \alpha_n \equiv \epsilon/(a_+ T_n^4)$. Substituting these relations into Eqs. (29) and (21), one obtains [70]

$$\bar{\mathcal{P}}_{\text{LTE}} = a_+ T_n^4 f(\xi_w, \alpha_n), \quad (33)$$

where

$$f(\xi_w, \alpha_n) = -\frac{2\gamma_w^2}{9} \left[1 - 3\alpha_n + 3(\alpha_n - 1)\xi_w^2 + \sqrt{[1 - 3\alpha_n + 3(1 + \alpha_n)\xi_w^2]^2 - 12\xi_w^2} \right]. \quad (34)$$

Since in deriving $f(\xi_w, \alpha_n)$, one has used the matching condition (28), for given α_n this expression is valid only for the particular values of ξ_w that satisfy $\bar{\mathcal{P}}_{\text{LTE}} = \mathcal{P}_{\text{driving}}$. Alternatively, one can view ξ_w as a free variable but α_n as an implicit function of ξ_w defined by $\bar{\mathcal{P}}_{\text{LTE}} = \mathcal{P}_{\text{driving}}$. From this perspective, $\alpha_n(\xi_J)$ defines $\alpha_{n,\text{max}}^{\text{det}}$.

The Jouguet velocity ξ_J corresponds to $v_- = 1/\sqrt{3}$ [105]

$$\xi_J = \frac{1}{\sqrt{3}} \left(\frac{1 + \sqrt{3\alpha_n \left(\frac{2}{3} + \alpha_n \right)}}{1 + \alpha_n} \right). \quad (35)$$

At $\xi_w = \xi_J$, the square-root term in Eq. (34) is vanishing. Substituting $\xi_w = \xi_J$ into $f(\xi_w, \alpha_n)$, one obtains

$$f(\alpha_{n,\text{max}}^{\text{det}}) = \frac{2}{3} \frac{3(\alpha_{n,\text{max}}^{\text{det}})^2 + \alpha_{n,\text{max}}^{\text{det}} + (1 - \alpha_{n,\text{max}}^{\text{det}})\sqrt{3(\alpha_{n,\text{max}}^{\text{det}})^2 + 2\alpha_{n,\text{max}}^{\text{det}}}}{2\alpha_{n,\text{max}}^{\text{det}} + 1 - \sqrt{3(\alpha_{n,\text{max}}^{\text{det}})^2 + 2\alpha_{n,\text{max}}^{\text{det}}}}, \quad (36)$$

where we have replaced α_n with $\alpha_{n,\text{max}}^{\text{det}}$. One can approximate $f(\alpha_{n,\text{max}}^{\text{det}})$ with a linear function

$$f(\alpha_{n,\text{max}}^{\text{det}}) \approx 0.3 + 3.155\alpha_{n,\text{max}}^{\text{det}}. \quad (37)$$

Substituting Eq. (37) into Eq. (33), we obtain

$$\bar{\mathcal{P}}_{\text{LTE,det}}^{\text{max}}(\alpha_{n,\text{max}}^{\text{det}}) \approx a_+ T_n^4 (0.3 + 3.155\alpha_{n,\text{max}}^{\text{det}}). \quad (38)$$

This approximated expression should work well for $\alpha_{n,\text{max}}^{\text{det}} \gtrsim 0.2$. For very small $\alpha_{n,\text{max}}^{\text{det}}$, one should use the exact result obtained from Eq. (36).

For $-\Delta V_T$, we have

$$-\Delta V_T = \frac{a_+ T_n^4}{3} (1 - br^4), \quad (39)$$

where $r \equiv \gamma_w/\gamma_-$ and $b \equiv a_-/a_+$. Above, we have used the LTE matching condition (23). Substituting $v_- = 1/\sqrt{3}$, $\xi_w = \xi_J$ into r , one obtains

$$r_J^4(\alpha_n) \equiv r^4(\alpha_n)|_{v_-=1/\sqrt{3}, \xi_w=\xi_J} = \frac{(\alpha_n + 1)^4}{[2\alpha_n + 1 - \sqrt{\alpha_n(3\alpha_n + 2)}]^2} \xrightarrow{\alpha_n \rightarrow \infty} (7 + 4\sqrt{3})\alpha_n^2. \quad (40)$$

Therefore, $-\Delta V_T$ evaluated at $\xi_w = \xi_J$ is

$$(-\Delta V_T)|_{\xi_J}(\alpha_n) = a_+ T_n^4 \left(\frac{1}{3} - \frac{b(\alpha_n + 1)^4}{3[2\alpha_n + 1 - \sqrt{\alpha_n(3\alpha_n + 2)}]^2} \right) \xrightarrow{\alpha_n \rightarrow \infty} -\frac{b(7 + 4\sqrt{3})\alpha_n^2}{3} a_+ T_n^4. \quad (41)$$

Finally, the driving pressure is

$$\mathcal{P}_{\text{driving}}(\alpha_n) = a_+ T_n^4 \alpha_n. \quad (42)$$

The equation $-\Delta V_T|_{\xi_J}(\alpha_{n,\text{max}}^{\text{det}}) + \bar{\mathcal{P}}_{\text{LTE,det}}^{\text{max}}(\alpha_{n,\text{max}}^{\text{det}}) = \mathcal{P}_{\text{driving}}(\alpha_{n,\text{max}}^{\text{det}})$ gives

$$\begin{aligned} & \frac{b(\alpha_{n,\text{max}}^{\text{det}} + 1)^4}{\left[2\alpha_{n,\text{max}}^{\text{det}} + 1 - \sqrt{\alpha_{n,\text{max}}^{\text{det}}(3\alpha_{n,\text{max}}^{\text{det}} + 2)}\right]^2} + 3\alpha_{n,\text{max}}^{\text{det}} \\ &= 1 + 2 \frac{3(\alpha_{n,\text{max}}^{\text{det}})^2 + \alpha_{n,\text{max}}^{\text{det}} + (1 - \alpha_{n,\text{max}}^{\text{det}})\sqrt{3(\alpha_{n,\text{max}}^{\text{det}})^2 + 2\alpha_{n,\text{max}}^{\text{det}}}}{2\alpha_{n,\text{max}}^{\text{det}} + 1 - \sqrt{3(\alpha_{n,\text{max}}^{\text{det}})^2 + 2\alpha_{n,\text{max}}^{\text{det}}}}. \end{aligned} \quad (43)$$

For $b \rightarrow 1$, this can be approximated by [72]

$$\alpha_{n,\text{max}}^{\text{det}} \approx \frac{1-b}{3} \left(1 + \frac{4}{3} \sqrt{\frac{1-b}{6}}\right) \quad \text{for } b \rightarrow 1. \quad (44)$$

In Fig. 3 we show the comparison between the solution of Eq. (43) (blue solid line) and its approximation (44) (blue dashed line).

4.2 $\mu\nu$ -model

The analysis for the bag EoS can be generalized to the $\mu\nu$ -model [108], which is also called the ν -model in Ref. [109] and the template model in Refs. [72, 74, 110]. The $\mu\nu$ -model is a generalization of the bag model where the sound speed is allowed to deviate from $1/\sqrt{3}$. Explicitly, the EoS reads

$$e_s(T) = \frac{1}{3}a_+(\mu - 1)T^\mu + \epsilon, \quad p_s(T) = \frac{1}{3}a_+T^\mu - \epsilon, \quad (45)$$

$$e_b(T) = \frac{1}{3}a_-(\nu - 1)T^\nu, \quad p_b(T) = \frac{1}{3}a_-T^\nu, \quad (46)$$

where the constants μ, ν are related to the sound speed in the symmetric and broken phases through

$$\mu = 1 + \frac{1}{c_s^2}, \quad \nu = 1 + \frac{1}{c_b^2}. \quad (47)$$

In this case the two matching conditions (18a) and (28) have a more specific form [72]

$$\frac{v_+}{v_-} = \frac{v_+v_-(\nu - 1) - 1 + 3\alpha_+}{v_+v_-(\nu - 1) - 1 + 3v_+v_-\alpha_+}, \quad (48a)$$

$$v_+v_- = \frac{-\left(\frac{\gamma_+}{\gamma_-}\right)^\nu \Psi_+ + 1 - 3\alpha_+}{3\nu\alpha_+} [1 - (\nu - 1)v_+v_-], \quad (48b)$$

where

$$\alpha_+ = \alpha(T_+) \equiv \frac{\frac{1}{3}a_+(\mu - \nu)T_+^\mu + \nu\epsilon}{a_+\mu T_+^\mu}. \quad (49)$$

and Ψ is the ratio of the enthalpies in the broken and the symmetric phase

$$\Psi(T) \equiv \frac{\omega_b(T)}{\omega_s(T)} \quad (50)$$

such that

$$\Psi_+ \equiv \Psi(T_+) = \left(\frac{a_-}{a_+}\right) \left(\frac{\nu}{\mu}\right) T_+^{\nu-\mu}. \quad (51)$$

For $\mu = \nu = 4$, Ψ_+ becomes the parameter b , and α_+ becomes $\epsilon/(a_+ T_+^4)$.

In the detonation regime for the $\mu\nu$ -model, we have $\Psi_+ = \Psi_n \equiv (a_-/a_+)(\nu/\mu)T_n^{\nu-\mu}$. The Jouguet velocity is obtained by substituting $v_- = c_b$ into Eq. (48a) and reads [72, 109]

$$\xi_J = c_b \left(\frac{1 + \sqrt{3\alpha_n(1 - c_b^2 + 3c_b^2\alpha_n)}}{1 + 3c_b^2\alpha_n} \right). \quad (52)$$

For $c_b = 1/\sqrt{3}$, one recovers Eq. (35). Substituting the EoS into Eq. (21) and using $v_- = c_b$, $v_+ = \xi_J$, one obtains

$$\bar{\mathcal{P}}_{\text{LTE,det}}^{\text{max}} = a_+ T_n^\mu \left(\frac{\mu}{3} [\gamma(\xi_J)]^2 \xi_J (\xi_J - c_b) \right). \quad (53)$$

At the Jouguet point, $-\Delta V_T$ reads

$$(-\Delta V_T)|_{\xi_J} = \frac{a_+ T_n^\mu}{3} \left[1 - \Psi_n \left(\frac{\gamma(\xi_J)}{\gamma(c_b)} \right)^\nu \left(\frac{\mu}{\nu} \right) \right], \quad (54)$$

where we also used the LTE matching condition (23). The driving pressure reads

$$\mathcal{P}_{\text{driving}} = a_+ T_n^\mu \left[\frac{1}{3} + \left(\frac{\mu}{\nu} \right) \left(\alpha_n - \frac{1}{3} \right) \right]. \quad (55)$$

Equating $\mathcal{P}_{\text{LTE,det}}^{\text{max}}$ to $\mathcal{P}_{\text{driving}}$, one can obtain $\alpha_{n,\text{max}}^{\text{det}}$. For $\Psi_n \rightarrow 1$, one has the approximation [72]

$$\alpha_{n,\text{max}}^{\text{det}} \approx \frac{1 - \Psi_n}{3} \left(1 + \frac{\nu}{3} \sqrt{\frac{1 - \Psi_n}{(\nu - 1)(\nu - 2)}} \right) \quad \text{for } \Psi_n \rightarrow 1. \quad (56)$$

For $\mu = 4.1$, $\nu = 4.2$, we show the comparison between the exact result (red solid) and the approximation (red dashed) in Fig. 3. In the numerical result, we also observe that, different from the approximation (56), $\mathcal{P}_{\text{LTE,det}}^{\text{max}} = \mathcal{P}_{\text{driving}}$ can have a *detonation* solution for $\alpha_{n,\text{max}}^{\text{det}} > 0$ only when Ψ_n is smaller than a critical value $\Psi_{n,\text{crit}}$. For $\mu = 4.1, \nu = 4.2$, $\Psi_{n,\text{crit}} \approx 0.97619$. For $\mu = \nu = 4$, this critical value goes to one, as expected.

5 Maximal hydrodynamic obstruction

Now we generalize the analysis given in the last section to the hybrid regime and derive the maximal phase transition strength (for a given value of b or Ψ_n) that allows for non-runaway hybrid motions, $\alpha_{n,\text{max}}^{\text{hyb}}$. According to the discussion in Sec. 3, this also gives the critical

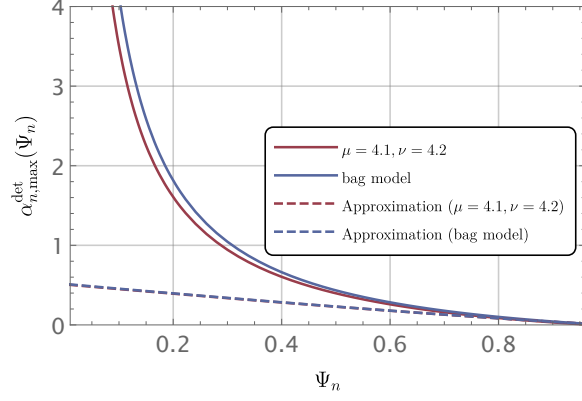


Figure 3: $\alpha_{n,\max}^{\text{det}}$ as a function of Ψ_n for the bag model ($\mu = \nu = 4$, blue line) and for $\mu = 4.1, \nu = 4.2$, and their approximations given in Eq. (56). The lines for the approximations almost overlap for the chosen values of ν .

phase transition strength above which the maximal LTE force can never balance out the driving force, i.e., $\alpha_{n,\text{crit}}^{\text{LTE}} = \alpha_{n,\max}^{\text{hyb}}$.

Below, we shall work with the $\mu\nu$ -model directly and the results for the bag model are obtained by taking $\mu = \nu = 4$. With this EoS and in the hybrid regime, we have

$$\bar{\mathcal{P}}_{\text{LTE}}^{\max} = a_+ T_+^\mu \left[\frac{\mu}{3} [\gamma(v_+)]^2 v_+ (v_+ - c_b) \right], \quad (57a)$$

$$(-\Delta V_T)|_{\xi_w = \xi_J} = \frac{a_+ T_+^\mu}{3} \left[1 - \left(\frac{\mu}{\nu} \right) \Psi_+ \left(\frac{\gamma(v_+)}{\gamma(c_b)} \right)^\nu \right], \quad (57b)$$

$$\mathcal{P}_{\text{driving}} = a_+ T_+^\mu \left[\frac{1}{3} + \left(\frac{\mu}{\nu} \right) \left(\alpha_+ - \frac{1}{3} \right) \right]. \quad (57c)$$

The common factor $a_+ T_+^\mu$ will be canceled out in the equation $\bar{\mathcal{P}}_{\text{LTE}}^{\max} = \mathcal{P}_{\text{driving}}$. Compared with the detonation regime, in the hybrid regime, we now have an additional shock wave. As a consequence, we do *not* have the good properties $v_+ = \xi_w$ and $T_+ = T_n$ ($\Rightarrow \alpha_+ = \alpha_n$, $\Psi_+ = \Psi_n$) anymore. One then needs to find the corresponding modified relations with the help of the matching conditions across the shock-wave front. Since $\bar{\mathcal{P}}_{\text{LTE}}^{\max}$ occurs nearly at ξ_J ,

$$\xi_w \approx \xi_J = c_b \left(\frac{1 + \sqrt{3\alpha_n(1 - c_b^2 + 3c_b^2\alpha_n)}}{1 + 3c_b^2\alpha_n} \right), \quad (58)$$

$\alpha_{n,\max}^{\text{hyb}}/\alpha_{n,\text{crit}}^{\text{LTE}}$ can be derived by considering an infinitely thin shock wave. For larger ξ_w , the shock wave disappears and the motion enters into the detonation regime.

We denote the hydrodynamic quantities on both sides of the shock-wave front *in the rest frame of the latter* as $T_{\text{sw},\pm}$, $v_{\text{sw},\pm}$. To understand the physics of the hydrodynamic obstruction, we first realize that the shock wave reheats the plasma to some temperature $T_{\text{sw},-} > T_n$. In principle, the fluid equations [105] should be integrated from $T_{\text{sw},-}$ to obtain the temperature right in front of the wall T_+ . However, as the velocity of the wall approaches the Jouguet velocity $\xi_w \rightarrow \xi_J$, the distance between the shock-wave front and the wall diminishes to zero and $T_{\text{sw},-} \rightarrow T_+$. So, to study the pressure at the peak, we can set $T_{\text{sw},-} = T_+$. We will see that T_+ becomes fixed as a function of α_n . Similarly, the fluid velocity right behind the shock-wave front $v_{\text{sw},-}$, and that right in front of the wall v_+ , when transformed to the common plasma frame, are also equal to each other for $\xi_w \rightarrow \xi_J$.

Therefore, we have

$$T_{\text{sw},+} = T_n, \quad v_{\text{sw},+} = \xi_{\text{sw}}, \quad T_{\text{sw},-} = T_+, \quad \bar{v}_{\text{sw},-} = \bar{v}_+, \quad (59)$$

where ξ_{sw} is the velocity of the shock-wave front, and a bar indicates that the quantity is transformed to the plasma frame:⁵

$$\bar{v}_{\text{sw},-} \equiv \frac{\xi_{\text{sw}} - v_{\text{sw},-}}{1 - \xi_{\text{sw}} v_{\text{sw},-}}, \quad \bar{v}_+ \equiv \frac{\xi_w - v_+}{1 - \xi_w v_+}. \quad (60)$$

The last relation in Eq. (59) gives [70]

$$v_{\text{sw},-} = \frac{v_+ - \xi_w + \xi_{\text{sw}} - v_+ \xi_{\text{sw}} \xi_w}{1 + v_+ (\xi_{\text{sw}} - \xi_w) - \xi_w \xi_{\text{sw}}}, \quad \xi_{\text{sw}} > \xi_w. \quad (61)$$

With the $\mu\nu$ -model, we have the following matching conditions at the shock-wave front [72]

$$\xi_{\text{sw}} = c_s \sqrt{\frac{(\mu - 1) + \tilde{r}}{1 + (\mu - 1)\tilde{r}}}, \quad (62a)$$

$$v_{\text{sw},-} = \frac{c_s^2}{\xi_{\text{sw}}}, \quad (62b)$$

where

$$\tilde{r} \equiv \left(\frac{T_n}{T_+} \right)^\mu, \quad (\text{heating parameter}). \quad (63)$$

Looking at Eq.(62a), we observe that the maximal heating (smallest \tilde{r}) is obtained for the largest ξ_{sw} reachable. Furthermore, one can show that

$$\alpha_+ = \frac{\mu - \nu}{3\mu} + \left(\alpha_n - \frac{\mu - \nu}{3\mu} \right) \tilde{r}, \quad (64a)$$

$$\Psi_+ = \Psi_n \tilde{r}^{1-\nu/\mu}. \quad (64b)$$

Combining Eqs. (61) and (62b) gives

$$\frac{c_s^2}{\xi_{\text{sw}}} = \frac{v_+ - \xi_w + \xi_{\text{sw}} - v_+ \xi_{\text{sw}} \xi_w}{1 + v_+ (\xi_{\text{sw}} - \xi_w) - \xi_w \xi_{\text{sw}}}. \quad (65)$$

This relation can be used to show that the velocity of the shock-wave front is an increasing function of ξ_w , which means in turn that \tilde{r} decreases (the heating increases) for a larger ξ_w , until the shock wave disappears at the Jouguet velocity. We thus confirm here that the peak in the pressure (due to heating) is located at the Jouguet velocity. Finally, v_+ can be eliminated by substituting $v_- = c_b$ into the matching conditions (18a) and (28) giving⁶

$$v_+ = c_b \left(\frac{1 - \sqrt{3\alpha_+ (1 - c_b^2 + 3c_b^2 \alpha_+)}}{1 + 3c_b^2 \alpha_+} \right). \quad (66)$$

Substituting Eqs. (58), (62a), (64a) and (66) into Eq. (65), one gets an algebraic equation for \tilde{r} and α_n . After obtaining $\tilde{r}(\alpha_n)$, one also numerically obtains $\{v_+, \xi_w, \xi_{\text{sw}}, \alpha_+\}$ in terms of α_n . Substituting them into Eq. (57a) and rewriting α_n as $\alpha_{n,\text{crit}}^{\text{LTE}}$, we then obtain $\bar{\mathcal{P}}_{\text{LTE}}^{\text{max}}(\alpha_{n,\text{crit}}^{\text{LTE}})/(a_+ T_+^\mu)$. Together with Eq. (64b), we can also obtain $(-\Delta V_T)/(a_+ T_+^\mu)$, $\mathcal{P}_{\text{driving}}/(a_+ T_+^\mu)$ in terms of α_n . Finally, the equation $\mathcal{P}_{\text{LTE}}^{\text{max}}(\alpha_{n,\text{crit}}^{\text{LTE}}) = \mathcal{P}_{\text{driving}}(\alpha_{n,\text{crit}}^{\text{LTE}})$ gives $\alpha_{n,\text{crit}}^{\text{LTE}}$ as a function of Ψ_n .

⁵Note that all the velocity quantities are defined in a way such that they are positive. This needs to be taken into account when taking the Lorentz transformation.

⁶Note the condition $v_+ < v_-$ for hybrids so that one needs to select the correct root for the quadratic equation of v_+ .

Bag equation of state. We apply this numerical procedure for $\mu = \nu = 4$ ($\Psi_n = b$ in this case) and show the result in Fig. 4 (left panel) where we also compare the obtained $\alpha_{n,\text{crit}}^{\text{LTE}}$ with $\alpha_{n,\text{max}}^{\text{det}}$ and its approximation (44). One can see that $\alpha_{n,\text{crit}}^{\text{LTE}}$ increases very fast as b decreases. Unless when b is very close to one, $\alpha_{n,\text{crit}}^{\text{LTE}}$ significantly differs from $\alpha_{n,\text{max}}^{\text{det}}$. We emphasize that $\alpha_{n,\text{crit}}^{\text{LTE}}(b)$ as a function of b is universal; it does not depend on the underlying particle physics model. Therefore, for the convenience of future applications, we provide the following fit, valid for $\mu = \nu = 4$,

$$\alpha_{n,\text{crit}}^{\text{LTE}}(b) \approx A + B(b - D)^C, \quad A = -0.1, \quad B = 0.014, \quad C = -1.3, \quad D = 0.77. \quad (67)$$

The comparison between the above fit and the numerical result is shown in the right panel of Fig. 4.

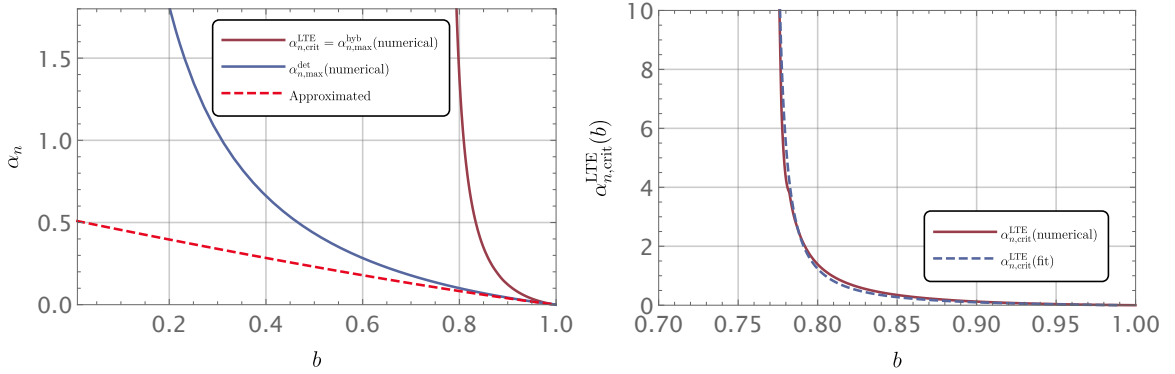


Figure 4: Left: Comparison between $\alpha_{n,\text{crit}}^{\text{LTE}}$, $\alpha_{n,\text{max}}^{\text{det}}$ and the approximation (44) for $\mu = \nu = 4$. Right: Comparison between the numerical $\alpha_{n,\text{crit}}^{\text{LTE}}$ and the fit given in Eq. (67).

Moreover, it seems that there is a critical value of b , around 0.77, where $\alpha_{n,\text{crit}}^{\text{LTE}}$ diverges. To clarify the physical significance of this divergence, we plot on the Left of Fig. 5 the value of the α_+ , as a function of α_n . This shows that *within the LTE approximation*, no matter how supercooled the phase transition is, in the limit of large α_n , the effective strength that the phase boundary feels goes to a constant $\alpha_+(\alpha_n \rightarrow \infty) \rightarrow 0.0668$. This means that using the equations for the driving pressure in Eq. (57), the driving force saturates, even for α_n going to infinity. On the Right of Fig. 5, we show that the driving force never reaches the friction for $b < 0.77$.

This result agrees with the numerical analysis presented in Ref. [72]. Since the peak in the pressure essentially comes from a heating effect in front of the bubble wall, which is absent in the limit of $\alpha_n \rightarrow \infty$, this result must be unphysical. The LTE approximation that we have followed should break down at some large value of α_n and the unphysical conclusion should be mitigated when the LTE approximation is replaced with an analysis in terms of microphysical particle processes with an exchange of momentum between the wall and the plasma. How exactly the LTE may break down as α_n increases is left for future work, but will be very briefly discussed in Sec. 7.

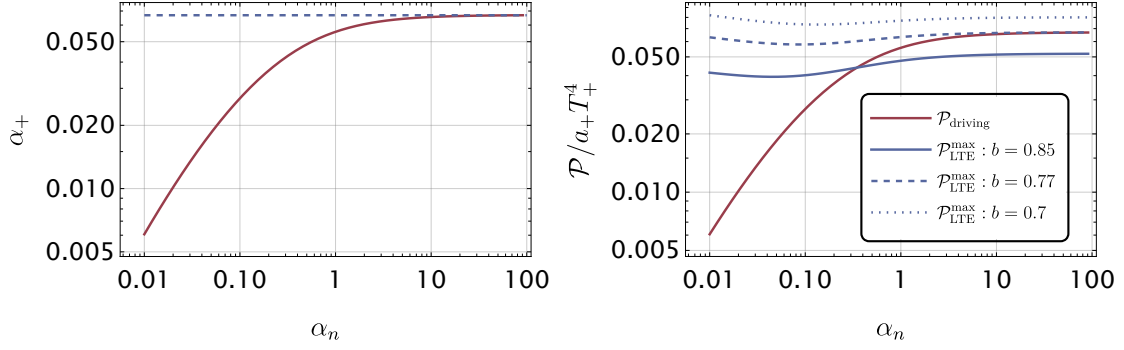


Figure 5: Left: Plot of α_+ as a function of α_n . We observe a saturation at $\alpha_+(\alpha_n \rightarrow \infty) \rightarrow 0.0668$. This saturation indicates that from the point of view of the phase boundary, the effective phase transition strength saturates as we increase α_n . Right: Comparison between the driving and maximal LTE pressure on the bubble wall: When the maximal LTE friction (blue line) is always higher than the driving force (Red line), the heating prevents the runaway, for any α_n .

6 Comparison with the Bodeker-Moore criterion

The BM thermal frictional pressure is given in Eq. (2). This pressure is model dependent. Defining a characteristic energy scale M

$$M^2 \equiv \frac{\sum_i c_i g_i \Delta m_i^2}{\sum_i g_i}, \quad (68)$$

where the sum goes over the species that acquire a mass through the phase transition, Eq. (2) becomes

$$\mathcal{P}_{\text{BM}} \approx \frac{\Delta g_{\text{eff}} M^2 T_n^2}{24}, \quad (69)$$

where Δg_{eff} denotes the change in the number of relativistic DoFs in the plasma from the outside to the inside of the wall. We have assumed that the particles gaining mass have $m_i \gg T_-$ inside the wall such that they do not contribute to the relativistic DoFs after entering the bubble. To compare it with $\mathcal{P}_{\text{LTE}}^{\text{max}}$, we consider the bag EoS where $(a_+ - a_-) = \pi^2 \Delta g_{\text{eff}} / 30$ and we have

$$\mathcal{P}_{\text{BM}} \approx \frac{30 M^2 T_n^2 (a_+ - a_-)}{24 \pi^2} = \frac{5 M^2 T_n^2 (1 - b) a_+}{4 \pi^2}. \quad (70)$$

Therefore, we have the BM runaway criterion

$$\frac{5(1-b)}{4\pi^2} \left(\frac{M}{T_n} \right)^2 (a_+ T_n^4) < \alpha_n (a_+ T_n^4) \equiv \Delta V \quad \Rightarrow \quad \alpha_n > \frac{5(1-b)}{4\pi^2} \left(\frac{M}{T_n} \right)^2 \equiv \alpha_{n,\text{crit}}^{\text{BM}}, \quad (71)$$

where we have used the expression of the driving pressure in the bag EoS. The parameter M/T_n can be calculated once the particle physics model is given.

In the left panel of Fig. 6, we compare $\alpha_{n,\text{crit}}^{\text{LTE}}$ with $\alpha_{n,\text{crit}}^{\text{BM}}$ for $M/T_n = 2, 5, 10$. In the right panel of Fig. 6, taking $M/T_n = 5$ as an example, we show the modified runaway criterion. The dashed and dotted lines represent the BM and LTE runaway criteria, respectively. The solid line, which is obtained from $\max\{\alpha_{n,\text{crit}}^{\text{LTE}}, \alpha_{n,\text{crit}}^{\text{BM}}\}$, represents the modified runaway criterion. The shaded region gives a conservative estimate for the parameter space allowing

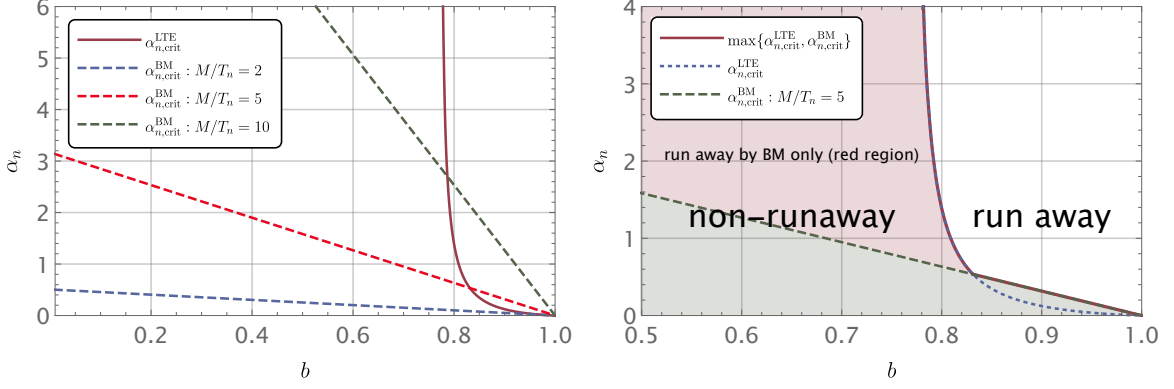


Figure 6: Left: Comparison between $\alpha_{n,\text{crit}}^{\text{LTE}}$ and $\alpha_{n,\text{crit}}^{\text{BM}}$ for $\mu = \nu = 4$ and $M/T_n = 2, 5, 10$. Right: Modified runaway curve obtained from $\max\{\alpha_{n,\text{crit}}^{\text{LTE}}, \alpha_{n,\text{crit}}^{\text{BM}}\}$, above which the bubble wall’s acceleration can be stopped by neither the hydrodynamic obstruction nor the leading-order BM thermal friction. All the shaded regions (red and green) give non-runaway walls by the modified criterion, while the red region would give runaway walls if hydrodynamic obstruction is not taken into account. Recall our comment below Eq. (3) on the term “runaway” used in this paper.

non-runaway walls. The large red region would be (incorrectly) estimated to give runaway walls if hydrodynamic obstruction is not taken into account, even in the non-supercooled regime $\alpha_n < 1$.

Note that for $\alpha_n < \alpha_{n,\text{crit}}^{\text{LTE}}$, the wall velocity is bounded by the Jouguet velocity, $\xi_w \leq \xi_J$. For a phenomenologically large α_n , e.g., $\alpha_n = 10$, $\gamma(\xi_J) \approx 7.64$, which is much smaller than the typical value of γ_w for the ultrarelativistic regime considered in Refs. [1, 75], $\gamma_w \sim 10^9$. Actually, the phase transition strength cannot be arbitrarily large, otherwise, the phase transition cannot complete [111]. This ensures that the LTE force becomes maximal typically before the wall enters the ultrarelativistic regime for practical phase transition strengths. Therefore, $\alpha_{n,\text{crit}}^{\text{LTE}}$ alone can serve as a criterion for whether the wall can enter into the ultrarelativistic regime or not, and thus is important for phenomenological studies involving ultrarelativistic walls. Let us now illustrate within an actual particle physics model, how to compute the hydrodynamic obstruction.

How to compute b in BSM models. We have seen that $b \equiv a_-/a_+$ is a crucial quantity for the determination of the hydrodynamic obstruction. Let us now discuss how to work out its value for BSM particle physics models, especially if the BSM sector is weakly coupled with the SM (as considered in, e.g., Ref. [112]). First of all, the matching conditions are based on the total energy-momentum conservation between the order-parameter scalar and the plasma. If some particle species do not respond to the passage of the wall quickly enough, they can be taken as completely “invisible” to the wall and they should not be taken into account when analyzing the total energy-momentum conservation. Therefore, a_+ should contain all the particles that couple directly/strongly to the bubble wall (that we call *active*) which give a contribution $a_{+, \text{active}}$. However, there are some particles that couple *indirectly* to the wall via the active particles (that we call *passive*) such that the exchange of energy/momentum between the active and the passive particles occurs on a length scale much smaller than the size of the perturbed fluid around the wall, which can be approximated by the bubble radius.⁷ These passive particles also need to be counted and

⁷MV thanks Benoit Laurent for very helpful discussions on this point.

give a contribution $a_{+, \text{passive}}$. Mathematically, we have

$$a_{+, \text{passive}} = \text{number of DoF with } R_{\text{bubble}} \gg L_{\text{therm}},$$

$$a_+ = a_{+, \text{active}} + a_{+, \text{passive}},$$

where L_{therm} is the length of thermalisation of the passive particles due to the exchange of energy/momentum between active and passive particles. In the opposite limit, particles coupling very weakly to active ones such that $R_{\text{bubble}} \ll L_{\text{therm}}$ can be fully ignored in the analysis. As an example, in the EWPT, the top quark would be an active particle, the electron would be a passive particle⁸ and the neutrino would be discarded in counting the DoFs. The quantity a_- is computed in the same way, with the further requirement that $m_- < T_-$. Since the passive particles do not couple to the order parameter, their DoFs do not change across the wall as long as the change in the temperature across the wall is not too big:

$$a_{+, \text{passive}} = a_{-, \text{passive}}. \quad (72)$$

Relevance for particle physics models and phenomenology. Let us quickly comment on a typical model where our discussion might be relevant. Spontaneous $B - L$ symmetry breaking is a physically motivated phase transition with a Lagrangian of the following form

$$\mathcal{L}_{\text{int}} = \frac{1}{2} \sum_I y_I \Phi \bar{N}_I^c N_I + \sum_{\alpha, I} Y_{D, \alpha I} H \bar{L}_\alpha N_I + h.c., \quad (73)$$

where L_α are the SM lepton doublets, N_I are the three families of heavy right-handed neutrinos, $Y_{D, \alpha I}$ are the *Dirac* Yukawa couplings between N_I and L_α , and y_I are *Majorana* Yukawa couplings. After the phase transition, $\langle \Phi \rangle = v_\phi / \sqrt{2}$ and the type-I seesaw Lagrangian is recovered with $M_I = \frac{1}{\sqrt{2}} y_I v_\phi$.

The phase transition $\langle \Phi \rangle = 0 \rightarrow v_\phi / \sqrt{2}$ can be strongly first order if Φ couples to gauge bosons and/or another scalar s via a coupling of the form $-\Delta \mathcal{L} = \frac{\lambda_{s\phi}}{2} s^2 |\Phi|^2$, inducing a mass $M_s^2(\phi) = \lambda_{s\phi} \phi^2$. It has been shown that the bubble wall induces an enhancement of the leptogenesis efficiency [44], which however strongly depends on the terminal velocity of the bubble wall. $b \equiv a_- / a_+$ can be computed in the following way: $(30/\pi^2) a_{+, \text{active}} = 6 + 2 + 1 = 9$ (assuming three families of RH, one complex Φ and a singlet s), and $(30/\pi^2) a_{-, \text{active}} \approx 1$. $a_{+, \text{passive}}$ is more delicate to compute and depends on the value of $Y_{D, \alpha I}$. The N_I couple to the SM via the couplings $Y_{D, \alpha I}$ and the typical length scale for thermalisation between N_I (active particles) and SM particles, typically via Higgs-mediated $NL \rightarrow NL$, is given by [113]

$$L_{\text{therm}}^{-1} \equiv \langle \sigma_{NL \rightarrow NL} v \rangle n_L \sim Y_D^4 \frac{T_n}{8\pi^3}. \quad (74)$$

Within our model, we have

$$Y_D^2 \sim 10^{-12} \frac{M_I}{10^3 \text{GeV}}, \quad L_{\text{therm}} \sim \frac{10^{25}}{T_n} \left(\frac{10^3 \text{GeV}}{M_I} \right)^2, \quad R_{\text{max}} \sim \frac{M_p}{10\beta v^2}, \quad (75)$$

⁸In this example, the electron does interact with the Higgs directly. But this direct Yukawa coupling is very small and hence can be ignored. However, the electron can interact with Higgs efficiently via the weak interactions.

where R_{max} is the bubble radius at collision. For $v_\phi \sim M_I \sim T_n \sim 10^{10}$ GeV, we can see that

$$L_{\text{therm}} \sim 10\text{GeV}^{-1}, \quad R_{\text{max}} \sim 0.01/\beta \text{ GeV}^{-1} \quad \Rightarrow \quad a_{+, \text{passive}} = a_{-, \text{passive}} = 0. \quad (76)$$

So under perturbation, the SM particles never thermalise within a scale shorter than the bubble scale. We obtain finally $b \sim 0.1$, which is a value that, according to the modified criterion, would not allow for runaway. In this case, we could approximate $\xi_w \approx \xi_J$.

7 Comments on the validity of our approximations

We have seen that the hydrodynamic obstruction is essentially a consequence of the strong heating of the plasma due to the shock wave in front of the wall. For this heating to occur, we however have to fulfil some conditions on hydrodynamics and exchange of energy. In this section, we would like to discuss a few possible weaknesses of our results, for the purpose of further studies.

- **The hydrodynamic regime:** We would like to emphasize that in this paper, our computation relied on hydrodynamics, which is by definition valid for scales much larger than the mean free path of particles in the plasma. For example, for a gauge theory with coupling g , the mean free path of the particles coupling to the gauge field would be [113]

$$L_{\text{MFP}} \equiv \frac{1}{\langle \sigma_{2 \rightarrow 2} v \rangle n_{\text{scatterers}}} \propto \frac{1}{g^4 T_n} = \mathcal{O}(1) \times \left(\frac{\alpha_n}{\Delta V} \right)^{1/4} \frac{1}{g^4}, \quad (77)$$

which we evaluated at the nucleation temperature. As we have seen, in the LTE picture, the pressure as a function of the velocity is not a monotonic function, but features a peak in the pressure at $\xi_{\text{peak}} \sim \xi_J$, which is related to α_n via Eq. (35) for the bag EoS. This means that for $\alpha_n \gg 1$, $\gamma(\xi_{\text{peak}}) \sim \mathcal{O}(1)\alpha_n^{1/2}$.

For our picture to hold, the hydrodynamic regime must be already valid when the velocity of the bubble wall becomes of the order of the velocity at the peak. Let us recall that the bubble nucleates at a microscopic scale, with an initial radius $R_{\text{initial}} \sim 1/T_n$ and then accelerates (assuming no initial obstruction from the plasma), via $\gamma_w \propto R/R_{\text{initial}}$. This implies that the velocity at the peak of the pressure ξ_{peak} is in principle already reached in the very early stage of the expansion, when $R \sim \text{few} \times R_{\text{initial}}$, for scales where it is not ensured that the hydrodynamic approximation is already valid. Roughly speaking, the bubble wall should enter the hydrodynamic regime when⁹

$$R \gg L_{\text{MFP}} \quad (\text{hydrodynamic criterion}), \quad (78)$$

where L_{MFP} is the mean free path of the active particles (the particles *interacting strongly with the wall*; in the case of the EWPT, they would be the top, W, Z, Higgs). If this criterion is not fulfilled, the LTE picture may not capture faithfully the pressure

⁹This type of worry can be circumvented in the case of a *monotonically* increasing pressure because for that case only the steady state would matter. More specifically, for a monotonically increasing pressure, the velocity at which the total pressure crosses zero is an attractor such that for a velocity either larger or smaller than that point, it will be pushed back to that value in the end when the hydrodynamic criterion $R \gg L_{\text{MFP}}$ is satisfied. We stress that this is not the case for a non-monotonous pressure.

on the wall and the collisionless picture seems to be the most relevant. It is however a nontrivial case-by-case study that we cannot do in full generality here.

We can however work out the trend. Since the peak in the bubble wall pressure exists only due to hydrodynamic effects. For the criterion in Eq. (78) to be valid at the Jouguet velocity, this requires

$$\mathcal{O}(1)\gamma(\xi_J) \gtrsim 1/g^4 \quad \Rightarrow \quad \mathcal{O}(1)\alpha_n^{1/2} \gtrsim 1/g^4. \quad (79)$$

This suggests that hydrodynamics at the Jouguet velocity is valid for strongly coupled theories $g \sim 1$, like the strong coupling for the SM, and, perhaps surprisingly, for large supercooling.

This issue can be understood in another way, from the particle physics perspective. We have seen that the hydrodynamic obstruction disappears if the bubble wall manages to become a detonation. On the other hand, the hydrodynamic obstruction originates from the heating of the plasma due to the particles bouncing off the wall. For the hydrodynamic obstruction to be relevant in the early stage of the bubble wall, the time scale of the heating, t_{heating} , needs to be smaller than the time scale for the bubble wall to accelerate to the Jouguet velocity, $t_{\text{acceleration}}$:

$$t_{\text{acceleration}} \gg t_{\text{heating}}. \quad (80)$$

- **The self-similar solution** Even in the regime of validity of hydrodynamics, there is no guarantee that the peak in the pressure will manifest. Indeed, the picture presented in this paper relied on *self-similar solutions for the temperature and bulk velocity profiles*. It is known that such self-similarity profiles are reached asymptotically when $R \gg R_{\text{initial}}$. However, in the early stage of the bubble wall, the temperature profile might differ substantially from the self-similar solution. This would occur if the time scales of adaptation of the profile is much longer than the timescale of acceleration of the bubble.¹⁰ Verifying the validity of the self-similar profile or the real “existence” of the pressure peak, requires dynamical simulation, a study that we will perform in a forthcoming study [114].

8 Conclusion

In this paper, we have studied the criterion for the runaway behaviour of bubble walls within two opposite approximations: the ballistic approximation and the LTE approximation. These two approximations are usually applied to the ultrarelativistic regime and the relatively lower velocity regime, respectively. The former corresponds to the BM thermal friction and the latter corresponds to the hydrodynamic obstruction. These frictions thus typically exist in different regions of the wall velocity space. For both approximations, we formulate a different runaway criterion in terms of a critical phase transition strength, $\alpha_{n,\text{crit}}^{\text{BM/LTE}}$. For $\alpha_n > \alpha_{n,\text{crit}}^{\text{BM/LTE}}$, the acceleration of the wall cannot be stopped by the friction under study. The BM criterion for runaway walls $\alpha_{n,\text{crit}}^{\text{BM}} < \alpha_n$, valid within the ballistic approximation, has been widely used in the literature.

However, the BM criterion implicitly assumes that the friction is a monotonous function of the wall velocity. This is however not true and the hydrodynamic obstruction gives a pressure barrier before the wall enters into the ultrarelativistic regime [57, 58, 72]. The

¹⁰MV thanks Ryusuke Jinno for enlightening discussions on this point.

modified criterion on runaway when the hydrodynamic obstruction is taken into account should be $\alpha_n > \max\{\alpha_{n,\text{crit}}^{\text{BM}}, \alpha_{n,\text{crit}}^{\text{LTE}}\}$. While both $\alpha_{n,\text{crit}}^{\text{BM}}$ and $\alpha_{n,\text{crit}}^{\text{LTE}}$ depend on the ratio of the number of DoFs in the symmetry and broken phases b , $\alpha_{n,\text{crit}}^{\text{BM}}$ further depends on a particle physics model-dependent parameter, the ratio between the averaged mass gain and the nucleation temperature M/T_n . Therefore, $\max\{\alpha_{n,\text{crit}}^{\text{BM}}, \alpha_{n,\text{crit}}^{\text{LTE}}\}$ depends on the interplay of these two parameters. We have compared $\alpha_{n,\text{crit}}^{\text{BM}}$ with $\alpha_{n,\text{crit}}^{\text{LTE}}$ for some typical values of the model-dependent parameter M/T_n (cf. Fig. 6). We have argued that the BM is not always a sufficient criterion for the runaway (even in the absence of other sources of friction due to, e.g., $1 \rightarrow 2$ processes). In Sec. 5, Eq. (67), we provide easily implementable expressions for the maximal LTE pressure and we emphasize the fact that $\alpha_{n,\text{crit}}^{\text{LTE}}(b)$ *does not* depend on the particularities of the underlying particle physics model. It appears that within the LTE approximation, theories with large enough change in DoF, $b < 0.77$, have typically non-runaway walls due to the hydrodynamic obstruction. This would reduce drastically the region of parameter space allowing for runaway. Furthermore, $\alpha_{n,\text{crit}}^{\text{LTE}}$ is the lower bound for the phase transition strength that the wall can enter the ultrarelativistic regime and thus is a very important quantity for phenomenological studies involving ultrarelativistic walls.

We note that in this paper we have ignored other sources of friction that may exist. For the hydrodynamic obstruction, we have ignored out-of-equilibrium effects. For the BM criterion, we have ignored other sources of friction due to other particle physics processes. As a consequence, both $\alpha_{n,\text{crit}}^{\text{LTE}}$ and $\alpha_{n,\text{crit}}^{\text{BM}}$ serve as a most conservative estimate of the maximal phase transition strength under which non-runaway stationary walls can exist.

We also attract the attention to several caveats that may change our conclusions. Specifically, the velocity at which the hydrodynamic obstruction is maximal, ξ_J , is relatively low and can be reached at the early stage of the bubble expansion. Whether the approximations or assumptions used in this paper, i.e., the LTE approximation, hydrodynamics, and the self-similarity used for the plasma temperature and velocity profiles, are valid or not in such an early stage needs further investigation. We hope that our work can serve as a motivation to study the dynamical evolution of the bubble wall, not only its steady states, an investigation that we will initiate in Ref. [114].

Acknowledgments

The authors would like to thank Benoit Laurent, Simone Blasi, Jorinde Van de Vis, Carlos Tamarit and Aleksandr Azatov for clarifying discussions, as well as Ryusuke Jinno and Giulio Barni for comments on the draft. The work of WYA is supported by the Engineering and Physical Sciences Research Council (grant No. EP/V002821/1). XN is supported by the iBOF “Un-locking the Dark Universe with Gravitational Wave Observations: from Quantum Optics to Quantum Gravity” of the Vlaamse Interuniversitaire Raad. MV is supported by the “Excellence of Science - EOS” - be.h project n.30820817, and by the Strategic Research Program High-Energy Physics of the Vrije Universiteit Brussel.

A Discussion on the departure from LTE

In the main text, we have always assumed LTE and neglected the increase of entropy at the phase boundary. In this appendix, we try to broaden this picture and discuss what the increase of entropy would change.

Modification in the matching conditions. The first modification would appear in the relation between the pressure and the potential [70]

$$p(\phi, T) = -V_{\text{eff}}(\phi, T) + \delta p = -V(\phi) - V_T(\phi, T) + \delta p \equiv \bar{p}(\phi, T) + \delta p, \quad (81)$$

where δp encodes the out-of-equilibrium effects. We have introduced $\bar{p} \equiv -V(\phi) - V_T(\phi, T)$ to denote the equilibrium part of the pressure. In this notation, the p in the main text should be replaced with \bar{p} . With this additional δp , the matching condition in Eq. (18b) is modified to (assuming stationary motion for simplicity for the present discussion)

$$\omega_+ \gamma_+^2 v_+^2 + p_+ = \omega_- \gamma_-^2 v_-^2 + p_- \Rightarrow \Delta V = \Delta(-V_T + \omega \gamma^2 v^2 + \delta p). \quad (82)$$

Then one can identify the friction as

$$\mathcal{P}_{\text{friction}} = \mathcal{P}_{\text{LTE}} + \Delta \delta p, \quad (83)$$

where \mathcal{P}_{LTE} is defined as previously. Comparing it with Eq. (12), one then has

$$\begin{aligned} \Delta \delta p = \mathcal{P}_{\text{dissipative}} &= - \int_{-\delta}^{\delta} dz (\partial_z \phi) \left(\sum_i \frac{dm_i^2(\phi)}{d\phi} \int \frac{d^3 \mathbf{p}}{(2\pi)^3 2E_i} \delta f_i(p, z) \right), \\ \Rightarrow \frac{d\delta p}{dz} &= -(\partial_z \phi) \left(\sum_i \frac{dm_i^2(\phi)}{d\phi} \int \frac{d^3 \mathbf{p}}{(2\pi)^3 2E_i} \delta f_i(p, z) \right). \end{aligned} \quad (84)$$

The above equation can be used to compute δp from δf_i , the out-of-equilibrium part of the distribution functions.

Allowing for out-of-equilibrium, thermodynamic identities may be spoiled as there is no well-defined temperature for δf_i . We will assume a close-to-equilibrium system such that $\delta f_i \equiv f - f_i^{\text{eq}} \ll f_i^{\text{eq}}$ so that we still use f_i^{eq} to define most thermodynamic quantities except the additional δp in the pressure. In this sense, only the very direct effects on the friction of the wall are considered. Then,

$$e(\phi, T) = -\bar{p}(\phi, T) + T \frac{\partial \bar{p}(\phi, T)}{\partial T}, \quad (85)$$

as defined in LTE, and the entropy density is defined as $s = \omega/T = (e + \bar{p})/T$.

Although the entropy density is defined as previously, the presence of the deviation from equilibrium can induce the entropy production such that the matching condition Eq. (22) is modified by the introduction of a parameter Δs :

$$(s_+ + \Delta s) \gamma_+ v_+ = s_- \gamma_- v_-. \quad (86)$$

Using Eq. (18a), it can also be written as

$$\frac{T_+}{T_-} = \frac{\gamma_-}{\gamma_+} \left(1 + \frac{\Delta s}{s_+} \right). \quad (87)$$

It is clear that the parameters Δs and δp are in principle computable within a particle physics model and are related to each other. However, the computation of those parameters from a specific particle physics model is beyond the scope of this work. We leave it for future work.

Consequence of the entropy increase. For $-\Delta V_T$, we have

$$-\Delta V_T = \frac{a_+ T_+^4}{3} \left(1 - \frac{br^4}{(1 + \Delta s/s_+)^4} \right), \quad (88)$$

and thus the different contribution of the pressure in Eq. (57) becomes

$$\bar{\mathcal{P}}_{\text{LTE}}^{\text{max}} = a_+ T_+^\mu \left[\frac{\mu}{3} [\gamma(v_+)]^2 v_+ (v_+ - c_b) \right], \quad (89a)$$

$$(-\Delta V_T)|_{\xi_w=\xi_J} = \frac{a_+ T_+^\mu}{3} \left[1 - \left(\frac{\mu}{\nu} \right) \frac{\Psi_+}{(1 + \Delta s/s_+)^4} \left(\frac{\gamma(v_+)}{\gamma(c_b)} \right)^\nu \right], \quad (89b)$$

$$\mathcal{P}_{\text{driving}} = a_+ T_+^\mu \left[\frac{1}{3} + \left(\frac{\mu}{\nu} \right) \left(\alpha_+ - \frac{1}{3} \right) \right]. \quad (89c)$$

The consequence of the entropy injection is to lower the effective value of the parameter b by

$$b \rightarrow \frac{b}{(1 + \Delta s/s_+)^4}, \quad \Psi_+ \rightarrow \frac{\Psi_+}{(1 + \Delta s/s_+)^4}. \quad (90)$$

This effectively increases the frictional pressure on the bubble wall, since $(1 + \Delta s/s_+) > 1$.

Assuming that $\mathcal{P}_{\text{dissipative}}$, i.e., $\Delta \delta p$, is positive, one would confirm the idea that the LTE limit $\delta p \rightarrow 0, \Delta s \rightarrow 0$, gives a *lower* bound on the pressure. Once δp (or $\Delta \delta p$) is expressed in terms of $\Delta s/s_+$, then $\Delta s/s_+$ can be an additional parameter for hydrodynamic simulations. This is similar to that although α_n is computed from specific particle physics models, it is treated as a parameter in fluid dynamics [115].

$\Delta \delta p$ in the ultrarelativistic regime. One may get a feeling about $\Delta \delta p$ by considering the ultrarelativistic regime $\gamma_w \gg 1$. In this regime, we can use the collisionless/ballistic approximation. Then

$$\delta f_i = f_i - f_i^{\text{eq}}(z; T(z)) = f_i^{\text{in}}(T_+) - f_i^{\text{eq}}(z; T(z)) = \frac{1}{e^{|\mathbf{p}|/T_+} \pm 1} - \frac{1}{e^{\sqrt{\mathbf{p}^2 + m^2(z)}/T(z)} \pm 1} > 0 \quad (91)$$

when assuming $T_+ \approx T(z)$. The signs \pm correspond to the case of fermions/bosons entering the wall. Above f_i^{in} are the distribution functions for the incoming particles. In the collisionless limit, the distribution functions f_i do *not* depend on z because there are no interactions to change the plasma distribution so that the latter remains unchanged after the plasma passes through the wall. This is very similar to the $\Gamma \ll H$ limit (with Γ and H being the scattering rate of dark matter and the Hubble rate, respectively) in the freeze-out process that occurs however for the time-dependence of f_i instead of the z -dependence discussed here. We thus obtain

$$\Delta \delta p = \mathcal{P}_{\text{dissipative}} = - \sum_i \int_{-\delta}^{\delta} dz \underbrace{\frac{dm_i^2(\phi(z))}{dz}}_{<0} \underbrace{\left(\int \frac{d^3 \mathbf{p}}{(2\pi)^3 2E_i} \delta f_i \right)}_{>0} > 0. \quad (92)$$

This shows that $\Delta \delta p$ adds more friction to the wall.

Outside of the ultrarelativistic regime, one might expect $f_i(z) \in [f_i^{\text{in}}(T_+), f_i^{\text{eq}}(z; T(z))]$ and $f_i^{\text{in}} \approx f_i^{\text{in;eq}}$. Assuming $T_+ \sim T(z)$, one again has $\delta f_i(z) \geq 0$ due to the suppression from the masses in $f_i^{\text{eq}}(z; T(z))$ compared with $f_i^{\text{in;eq}}(T_+)$. Thus, both $\Delta \delta p$ and Δs increase

the resistance from the plasma on the wall expansion. The limit $\Delta\delta p \rightarrow 0$ and $\Delta s \rightarrow 0$ is indeed a lower bound on the pressure.

Further, in the ultrarelativistic regime we have $T_+ = T_n$ and $f_i^{\text{in}} = f_i^{\text{in;eq}}$ (incoming particles are in thermal equilibrium at the nucleation temperature). Then one can recognize

$$\begin{aligned} \Delta\delta p = & - \sum_i \int_{-\delta}^{\delta} dz \frac{dm_i^2(\phi(z))}{dz} \left(\int \frac{d^3\mathbf{p}}{(2\pi)^3 2E_i} f_i^{\text{in;eq}}(p; T_n) \right) \\ & + \sum_i \int_{-\delta}^{\delta} dz \frac{dm_i^2(\phi(z))}{dz} \left(\int \frac{d^3\mathbf{p}}{(2\pi)^3 2E_i} f_i^{\text{eq}}(p, z; T(z)) \right) = \mathcal{P}_{\text{BM}} - \mathcal{P}_{\text{LTE}}. \end{aligned} \quad (93)$$

This confirms that, for $\gamma_w \gg 1$, $\mathcal{P}_{\text{friction}} = \mathcal{P}_{\text{LTE}} + \mathcal{P}_{\text{dissipative}} \rightarrow \mathcal{P}_{\text{BM}}$. Note that one in general does *not* have $\mathcal{P}_{\text{LTE}} + \mathcal{P}_{\text{dissipative}} = \mathcal{P}_{\text{BM}}$ outside of the ultrarelativistic regime so that one cannot conclude that \mathcal{P}_{BM} is bigger than \mathcal{P}_{LTE} based on $\mathcal{P}_{\text{dissipative}} > 0$. To have $\mathcal{P}_{\text{friction}} = \mathcal{P}_{\text{BM}}$, we have assumed (i) f_i take the form of Eq. (91); (ii) the particles in front of the wall are in thermal equilibrium; and (iii) $T_+ = T_n$. When any of these assumptions are not satisfied, one cannot conclude $\mathcal{P}_{\text{friction}} = \mathcal{P}_{\text{BM}}$. In particular, in the presence of the heating effects, $T_+ > T_n$, and thus even when the other two assumptions are satisfied, we have $\mathcal{P}_{\text{LTE}} + \mathcal{P}_{\text{dissipative}} > \mathcal{P}_{\text{BM}}$.

References

- [1] D. Bodeker and G. D. Moore, “Can electroweak bubble walls run away?,” *JCAP* **05** (2009) 009, [arXiv:0903.4099 \[hep-ph\]](#).
- [2] E. Witten, “Cosmic Separation of Phases,” *Phys. Rev. D* **30** (1984) 272–285.
- [3] A. Kosowsky, M. S. Turner, and R. Watkins, “Gravitational radiation from colliding vacuum bubbles,” *Phys. Rev. D* **45** (1992) 4514–4535.
- [4] A. Kosowsky and M. S. Turner, “Gravitational radiation from colliding vacuum bubbles: envelope approximation to many bubble collisions,” *Phys. Rev. D* **47** (1993) 4372–4391, [arXiv:astro-ph/9211004](#).
- [5] M. Kamionkowski, A. Kosowsky, and M. S. Turner, “Gravitational radiation from first order phase transitions,” *Phys. Rev. D* **49** (1994) 2837–2851, [arXiv:astro-ph/9310044](#).
- [6] M. Hindmarsh, S. J. Huber, K. Rummukainen, and D. J. Weir, “Gravitational waves from the sound of a first order phase transition,” *Phys. Rev. Lett.* **112** (2014) 041301, [arXiv:1304.2433 \[hep-ph\]](#).
- [7] C. Caprini *et al.*, “Science with the space-based interferometer eLISA. II: Gravitational waves from cosmological phase transitions,” *JCAP* **04** (2016) 001, [arXiv:1512.06239 \[astro-ph.CO\]](#).
- [8] C. Caprini *et al.*, “Detecting gravitational waves from cosmological phase transitions with LISA: an update,” *JCAP* **03** (2020) 024, [arXiv:1910.13125 \[astro-ph.CO\]](#).
- [9] NANOGrav Collaboration, G. Agazie *et al.*, “The NANOGrav 15 yr Data Set: Evidence for a Gravitational-wave Background,” *Astrophys. J. Lett.* **951** no. 1, (2023) L8, [arXiv:2306.16213 \[astro-ph.HE\]](#).
- [10] EPTA, InPTA: Collaboration, J. Antoniadis *et al.*, “The second data release from the European Pulsar Timing Array - III. Search for gravitational wave signals,” *Astron. Astrophys.* **678** (2023) A50, [arXiv:2306.16214 \[astro-ph.HE\]](#).

- [11] D. J. Reardon *et al.*, “Search for an Isotropic Gravitational-wave Background with the Parkes Pulsar Timing Array,” *Astrophys. J. Lett.* **951** no. 1, (2023) L6, [arXiv:2306.16215 \[astro-ph.HE\]](#).
- [12] H. Xu *et al.*, “Searching for the Nano-Hertz Stochastic Gravitational Wave Background with the Chinese Pulsar Timing Array Data Release I,” *Res. Astron. Astrophys.* **23** no. 7, (2023) 075024, [arXiv:2306.16216 \[astro-ph.HE\]](#).
- [13] V. A. Kuzmin, V. A. Rubakov, and M. E. Shaposhnikov, “On the Anomalous Electroweak Baryon Number Nonconservation in the Early Universe,” *Phys. Lett. B* **155** (1985) 36.
- [14] M. E. Shaposhnikov, “Baryon Asymmetry of the Universe in Standard Electroweak Theory,” *Nucl. Phys. B* **287** (1987) 757–775.
- [15] D. E. Morrissey and M. J. Ramsey-Musolf, “Electroweak baryogenesis,” *New J. Phys.* **14** (2012) 125003, [arXiv:1206.2942 \[hep-ph\]](#).
- [16] B. Garbrecht, “Why is there more matter than antimatter? Computational methods for leptogenesis and electroweak baryogenesis,” *Prog. Part. Nucl. Phys.* **110** (2020) 103727, [arXiv:1812.02651 \[hep-ph\]](#).
- [17] **LISA** Collaboration, P. Amaro-Seoane *et al.*, “Laser Interferometer Space Antenna,” [arXiv:1702.00786 \[astro-ph.IM\]](#).
- [18] **LIGO Scientific, Virgo** Collaboration, B. P. Abbott *et al.*, “Observation of Gravitational Waves from a Binary Black Hole Merger,” *Phys. Rev. Lett.* **116** no. 6, (2016) 061102, [arXiv:1602.03837 \[gr-qc\]](#).
- [19] V. Corbin and N. J. Cornish, “Detecting the cosmic gravitational wave background with the big bang observer,” *Class. Quant. Grav.* **23** (2006) 2435–2446, [arXiv:gr-qc/0512039](#).
- [20] S. Kawamura *et al.*, “The Japanese space gravitational wave antenna: DECIGO,” *Class. Quant. Grav.* **28** (2011) 094011.
- [21] X. Gong *et al.*, “Descope of the ALIA mission,” *J. Phys. Conf. Ser.* **610** no. 1, (2015) 012011, [arXiv:1410.7296 \[gr-qc\]](#).
- [22] **TianQin** Collaboration, J. Luo *et al.*, “TianQin: a space-borne gravitational wave detector,” *Class. Quant. Grav.* **33** no. 3, (2016) 035010, [arXiv:1512.02076 \[astro-ph.IM\]](#).
- [23] H. Kodama, M. Sasaki, and K. Sato, “Abundance of Primordial Holes Produced by Cosmological First Order Phase Transition,” *Prog. Theor. Phys.* **68** (1982) 1979.
- [24] S. W. Hawking, I. G. Moss, and J. M. Stewart, “Bubble Collisions in the Very Early Universe,” *Phys. Rev. D* **26** (1982) 2681.
- [25] J. Garriga, A. Vilenkin, and J. Zhang, “Black holes and the multiverse,” *JCAP* **02** (2016) 064, [arXiv:1512.01819 \[hep-th\]](#).
- [26] H. Deng and A. Vilenkin, “Primordial black hole formation by vacuum bubbles,” *JCAP* **12** (2017) 044, [arXiv:1710.02865 \[gr-qc\]](#).
- [27] C. Gross, G. Landini, A. Strumia, and D. Teresi, “Dark Matter as dark dwarfs and other macroscopic objects: multiverse relics?,” *JHEP* **09** (2021) 033, [arXiv:2105.02840 \[hep-ph\]](#).
- [28] M. J. Baker, M. Breitbach, J. Kopp, and L. Mitnacht, “Primordial Black Holes from

- First-Order Cosmological Phase Transitions,” [arXiv:2105.07481](#) [[astro-ph.CO](#)].
- [29] K. Kawana and K.-P. Xie, “Primordial black holes from a cosmic phase transition: The collapse of Fermi-balls,” *Phys. Lett. B* **824** (2022) 136791, [arXiv:2106.00111](#) [[astro-ph.CO](#)].
 - [30] J. Liu, L. Bian, R.-G. Cai, Z.-K. Guo, and S.-J. Wang, “Primordial black hole production during first-order phase transitions,” *Phys. Rev. D* **105** no. 2, (2022) L021303, [arXiv:2106.05637](#) [[astro-ph.CO](#)].
 - [31] T. H. Jung and T. Okui, “Primordial black holes from bubble collisions during a first-order phase transition,” [arXiv:2110.04271](#) [[hep-ph](#)].
 - [32] P. Huang and K.-P. Xie, “Primordial black holes from an electroweak phase transition,” *Phys. Rev. D* **105** no. 11, (2022) 115033, [arXiv:2201.07243](#) [[hep-ph](#)].
 - [33] M. Lewicki, P. Toczek, and V. Vaskonen, “Primordial black holes from strong first-order phase transitions,” *JHEP* **09** (2023) 092, [arXiv:2305.04924](#) [[astro-ph.CO](#)].
 - [34] Y. Gouttenoire and T. Volansky, “Primordial Black Holes from Supercooled Phase Transitions,” [arXiv:2305.04942](#) [[hep-ph](#)].
 - [35] M. J. Baker, J. Kopp, and A. J. Long, “Filtered Dark Matter at a First Order Phase Transition,” *Phys. Rev. Lett.* **125** no. 15, (2020) 151102, [arXiv:1912.02830](#) [[hep-ph](#)].
 - [36] D. Chway, T. H. Jung, and C. S. Shin, “Dark matter filtering-out effect during a first-order phase transition,” *Phys. Rev. D* **101** no. 9, (2020) 095019, [arXiv:1912.04238](#) [[hep-ph](#)].
 - [37] W. Chao, X.-F. Li, and L. Wang, “Filtered pseudo-scalar dark matter and gravitational waves from first order phase transition,” *JCAP* **06** (2021) 038, [arXiv:2012.15113](#) [[hep-ph](#)].
 - [38] T. Vachaspati, “Magnetic fields from cosmological phase transitions,” *Phys. Lett. B* **265** (1991) 258–261.
 - [39] M. O. Olea-Romacho, “Primordial Magnetogenesis in the Two-Higgs-doublet Model,” [arXiv:2310.19948](#) [[hep-ph](#)].
 - [40] J. M. Cline and K. Kainulainen, “Electroweak baryogenesis at high bubble wall velocities,” *Phys. Rev. D* **101** no. 6, (2020) 063525, [arXiv:2001.00568](#) [[hep-ph](#)].
 - [41] A. Azatov, M. Vanvlasselaer, and W. Yin, “Baryogenesis via relativistic bubble walls,” *JHEP* **10** (2021) 043, [arXiv:2106.14913](#) [[hep-ph](#)].
 - [42] I. Baldes, S. Blasi, A. Mariotti, A. Sevrin, and K. Turbang, “Baryogenesis via relativistic bubble expansion,” *Phys. Rev. D* **104** no. 11, (2021) 115029, [arXiv:2106.15602](#) [[hep-ph](#)].
 - [43] P. Huang and K.-P. Xie, “Leptogenesis triggered by a first-order phase transition,” *JHEP* **09** (2022) 052, [arXiv:2206.04691](#) [[hep-ph](#)].
 - [44] E. J. Chun, T. P. Dutka, T. H. Jung, X. Nagels, and M. Vanvlasselaer, “Bubble-assisted leptogenesis,” *JHEP* **09** (2023) 164, [arXiv:2305.10759](#) [[hep-ph](#)].
 - [45] A. Azatov, M. Vanvlasselaer, and W. Yin, “Dark Matter production from relativistic bubble walls,” *JHEP* **03** (2021) 288, [arXiv:2101.05721](#) [[hep-ph](#)].
 - [46] A. Azatov, G. Barni, S. Chakraborty, M. Vanvlasselaer, and W. Yin,

- “Ultra-relativistic bubbles from the simplest Higgs portal and their cosmological consequences,” *JHEP* **10** (2022) 017, [arXiv:2207.02230 \[hep-ph\]](#).
- [47] D. Borah, A. Dasgupta, and I. Saha, “Leptogenesis and dark matter through relativistic bubble walls with observable gravitational waves,” *JHEP* **11** (2022) 136, [arXiv:2207.14226 \[hep-ph\]](#).
 - [48] C. Caprini and D. G. Figueroa, “Cosmological Backgrounds of Gravitational Waves,” *Class. Quant. Grav.* **35** no. 16, (2018) 163001, [arXiv:1801.04268 \[astro-ph.CO\]](#).
 - [49] **LISA Cosmology Working Group** Collaboration, P. Auclair *et al.*, “Cosmology with the Laser Interferometer Space Antenna,” *Living Rev. Rel.* **26** no. 1, (2023) 5, [arXiv:2204.05434 \[astro-ph.CO\]](#).
 - [50] R. Roshan and G. White, “Using gravitational waves to see the first second of the Universe,” [arXiv:2401.04388 \[hep-ph\]](#).
 - [51] R. Jinno, H. Seong, M. Takimoto, and C. M. Um, “Gravitational waves from first-order phase transitions: Ultra-supercooled transitions and the fate of relativistic shocks,” *JCAP* **10** (2019) 033, [arXiv:1905.00899 \[astro-ph.CO\]](#).
 - [52] M. Lewicki and V. Vaskonen, “Gravitational waves from bubble collisions and fluid motion in strongly supercooled phase transitions,” *Eur. Phys. J. C* **83** no. 2, (2023) 109, [arXiv:2208.11697 \[astro-ph.CO\]](#).
 - [53] M. Dine, R. G. Leigh, P. Y. Huet, A. D. Linde, and D. A. Linde, “Towards the theory of the electroweak phase transition,” *Phys. Rev. D* **46** (1992) 550–571, [arXiv:hep-ph/9203203](#).
 - [54] B.-H. Liu, L. D. McLerran, and N. Turok, “Bubble nucleation and growth at a baryon number producing electroweak phase transition,” *Phys. Rev. D* **46** (1992) 2668–2688.
 - [55] G. D. Moore and T. Prokopec, “Bubble wall velocity in a first order electroweak phase transition,” *Phys. Rev. Lett.* **75** (1995) 777–780, [arXiv:hep-ph/9503296](#).
 - [56] G. D. Moore and T. Prokopec, “How fast can the wall move? A Study of the electroweak phase transition dynamics,” *Phys. Rev. D* **52** (1995) 7182–7204, [arXiv:hep-ph/9506475](#).
 - [57] J. M. Cline, A. Friedlander, D.-M. He, K. Kainulainen, B. Laurent, and D. Tucker-Smith, “Baryogenesis and gravity waves from a UV-completed electroweak phase transition,” *Phys. Rev. D* **103** no. 12, (2021) 123529, [arXiv:2102.12490 \[hep-ph\]](#).
 - [58] B. Laurent and J. M. Cline, “First principles determination of bubble wall velocity,” *Phys. Rev. D* **106** no. 2, (2022) 023501, [arXiv:2204.13120 \[hep-ph\]](#).
 - [59] Y. Bea, J. Casalderrey-Solana, T. Giannakopoulos, D. Mateos, M. Sanchez-Garitaonandia, and M. Zilhão, “Bubble wall velocity from holography,” *Phys. Rev. D* **104** no. 12, (2021) L121903, [arXiv:2104.05708 \[hep-th\]](#).
 - [60] I. Baldes, Y. Gouttenoire, and F. Sala, “String Fragmentation in Supercooled Confinement and Implications for Dark Matter,” *JHEP* **04** (2021) 278, [arXiv:2007.08440 \[hep-ph\]](#).
 - [61] F. Bigazzi, A. Caddeo, A. L. Cotrone, and A. Paredes, “Dark Holograms and Gravitational Waves,” *JHEP* **04** (2021) 094, [arXiv:2011.08757 \[hep-ph\]](#).

- [62] F. Bigazzi, A. Caddeo, T. Canneti, and A. L. Cotrone, “Bubble wall velocity at strong coupling,” *JHEP* **08** (2021) 090, [arXiv:2104.12817 \[hep-ph\]](#).
- [63] Y. Bea, J. Casallerrey-Solana, T. Giannakopoulos, A. Jansen, D. Mateos, M. Sanchez-Garitaonandia, and M. Zilhão, “Holographic bubbles with Jecco: expanding, collapsing and critical,” *JHEP* **09** (2022) 008, [arXiv:2202.10503 \[hep-th\]](#). [Erratum: *JHEP* **03**, 225 (2023)].
- [64] Z. Kang and J. Zhu, “Confinement Bubble Wall Velocity via Quasiparticle Determination,” [arXiv:2401.03849 \[hep-ph\]](#).
- [65] G. C. Dorsch, S. J. Huber, and T. Konstandin, “Bubble wall velocities in the Standard Model and beyond,” *JCAP* **12** (2018) 034, [arXiv:1809.04907 \[hep-ph\]](#).
- [66] S. Jiang, F. P. Huang, and X. Wang, “Bubble wall velocity during electroweak phase transition in the inert doublet model,” *Phys. Rev. D* **107** no. 9, (2023) 095005, [arXiv:2211.13142 \[hep-ph\]](#).
- [67] T. Konstandin and J. M. No, “Hydrodynamic obstruction to bubble expansion,” *JCAP* **02** (2011) 008, [arXiv:1011.3735 \[hep-ph\]](#).
- [68] M. Barroso Mancha, T. Prokopec, and B. Swiezewska, “Field-theoretic derivation of bubble-wall force,” *JHEP* **01** (2021) 070, [arXiv:2005.10875 \[hep-th\]](#).
- [69] S. Balaji, M. Spannowsky, and C. Tamarit, “Cosmological bubble friction in local equilibrium,” *JCAP* **03** (2021) 051, [arXiv:2010.08013 \[hep-ph\]](#).
- [70] W.-Y. Ai, B. Garbrecht, and C. Tamarit, “Bubble wall velocities in local equilibrium,” *JCAP* **03** no. 03, (2022) 015, [arXiv:2109.13710 \[hep-ph\]](#).
- [71] S.-J. Wang and Z.-Y. Yuwen, “Hydrodynamic backreaction force of cosmological bubble expansion,” *Phys. Rev. D* **107** no. 2, (2023) 023501, [arXiv:2205.02492 \[hep-ph\]](#).
- [72] W.-Y. Ai, B. Laurent, and J. van de Vis, “Model-independent bubble wall velocities in local thermal equilibrium,” [arXiv:2303.10171 \[astro-ph.CO\]](#).
- [73] T. Krajewski, M. Lewicki, and M. Zych, “Hydrodynamical constraints on bubble wall velocity,” [arXiv:2303.18216 \[astro-ph.CO\]](#).
- [74] M. Sanchez-Garitaonandia and J. van de Vis, “Prediction of the bubble wall velocity for a large jump in degrees of freedom,” [arXiv:2312.09964 \[hep-ph\]](#).
- [75] D. Bodeker and G. D. Moore, “Electroweak Bubble Wall Speed Limit,” *JCAP* **05** (2017) 025, [arXiv:1703.08215 \[hep-ph\]](#).
- [76] S. H  che, J. Kozaczuk, A. J. Long, J. Turner, and Y. Wang, “Towards an all-orders calculation of the electroweak bubble wall velocity,” *JCAP* **03** (2021) 009, [arXiv:2007.10343 \[hep-ph\]](#).
- [77] A. Azatov and M. Vanvlasselaer, “Bubble wall velocity: heavy physics effects,” *JCAP* **01** (2021) 058, [arXiv:2010.02590 \[hep-ph\]](#).
- [78] Y. Gouttenoire, R. Jinno, and F. Sala, “Friction pressure on relativistic bubble walls,” *JHEP* **05** (2022) 004, [arXiv:2112.07686 \[hep-ph\]](#).
- [79] W.-Y. Ai, “Logarithmically divergent friction on ultrarelativistic bubble walls,” *JCAP* **10** (2023) 052, [arXiv:2308.10679 \[hep-ph\]](#).
- [80] A. Azatov, G. Barni, R. Petrossian-Byrne, and M. Vanvlasselaer, “Quantisation Across Bubble Walls and Friction,” [arXiv:2310.06972 \[hep-ph\]](#).

- [81] P. Schwaller, “Gravitational Waves from a Dark Phase Transition,” *Phys. Rev. Lett.* **115** no. 18, (2015) 181101, [arXiv:1504.07263 \[hep-ph\]](#).
- [82] M. Aoki, H. Goto, and J. Kubo, “Gravitational Waves from Hidden QCD Phase Transition,” *Phys. Rev. D* **96** no. 7, (2017) 075045, [arXiv:1709.07572 \[hep-ph\]](#).
- [83] A. J. Helmboldt, J. Kubo, and S. van der Woude, “Observational prospects for gravitational waves from hidden or dark chiral phase transitions,” *Phys. Rev. D* **100** no. 5, (2019) 055025, [arXiv:1904.07891 \[hep-ph\]](#).
- [84] K. Agashe, P. Du, M. Ekhterachian, S. Kumar, and R. Sundrum, “Cosmological Phase Transition of Spontaneous Confinement,” *JHEP* **05** (2020) 086, [arXiv:1910.06238 \[hep-ph\]](#).
- [85] J. Halverson, C. Long, A. Maiti, B. Nelson, and G. Salinas, “Gravitational waves from dark Yang-Mills sectors,” *JHEP* **05** (2021) 154, [arXiv:2012.04071 \[hep-ph\]](#).
- [86] W.-C. Huang, M. Reichert, F. Sannino, and Z.-W. Wang, “Testing the dark SU(N) Yang-Mills theory confined landscape: From the lattice to gravitational waves,” *Phys. Rev. D* **104** no. 3, (2021) 035005, [arXiv:2012.11614 \[hep-ph\]](#).
- [87] F. R. Ares, M. Hindmarsh, C. Hoyos, and N. Jokela, “Gravitational waves from a holographic phase transition,” *JHEP* **21** (2020) 100, [arXiv:2011.12878 \[hep-th\]](#).
- [88] Z. Kang, J. Zhu, and S. Matsuzaki, “Dark confinement-deconfinement phase transition: a roadmap from Polyakov loop models to gravitational waves,” *JHEP* **09** (2021) 060, [arXiv:2101.03795 \[hep-ph\]](#).
- [89] M. Reichert, F. Sannino, Z.-W. Wang, and C. Zhang, “Dark confinement and chiral phase transitions: gravitational waves vs matter representations,” *JHEP* **01** (2022) 003, [arXiv:2109.11552 \[hep-ph\]](#).
- [90] E. Morgante, N. Ramberg, and P. Schwaller, “Gravitational waves from dark SU(3) Yang-Mills theory,” *Phys. Rev. D* **107** no. 3, (2023) 036010, [arXiv:2210.11821 \[hep-ph\]](#).
- [91] S. He, L. Li, Z. Li, and S.-J. Wang, “Gravitational Waves and Primordial Black Hole Productions from Gluodynamics,” [arXiv:2210.14094 \[hep-ph\]](#).
- [92] K. Fujikura, Y. Nakai, R. Sato, and Y. Wang, “Cosmological phase transitions in composite Higgs models,” *JHEP* **09** (2023) 053, [arXiv:2306.01305 \[hep-ph\]](#).
- [93] R. Pasechnik, M. Reichert, F. Sannino, and Z.-W. Wang, “Gravitational Waves from Composite Dark Sectors,” [arXiv:2309.16755 \[hep-ph\]](#).
- [94] G. C. Dorsch and D. A. Pinto, “Bubble wall velocities with an extended fluid Ansatz,” [arXiv:2312.02354 \[hep-ph\]](#).
- [95] G. C. Dorsch, S. J. Huber, and T. Konstandin, “A sonic boom in bubble wall friction,” *JCAP* **04** no. 04, (2022) 010, [arXiv:2112.12548 \[hep-ph\]](#).
- [96] G. C. Dorsch, S. J. Huber, and T. Konstandin, “On the wall velocity dependence of electroweak baryogenesis,” *JCAP* **08** (2021) 020, [arXiv:2106.06547 \[hep-ph\]](#).
- [97] A. Azatov, D. Barducci, and F. Sgarlata, “Gravitational traces of broken gauge symmetries,” *JCAP* **07** (2020) 027, [arXiv:1910.01124 \[hep-ph\]](#).
- [98] R. Jinno and M. Takimoto, “Probing a classically conformal b-l model with gravitational waves,” *Physical Review D* **95** (2016) 015020, <https://api.semanticscholar.org/CorpusID:118696959>.

- [99] L. Delle Rose, G. Panico, M. Redi, and A. Tesi, “Gravitational Waves from Supercool Axions,” *JHEP* **04** (2020) 025, [arXiv:1912.06139 \[hep-ph\]](#).
- [100] T. Prokopec, J. Rezacek, and B. Świeżewska, “Gravitational waves from conformal symmetry breaking,” *JCAP* **02** (2019) 009, [arXiv:1809.11129 \[hep-ph\]](#).
- [101] S. De Curtis, L. Delle Rose, and G. Panico, “Composite Dynamics in the Early Universe,” *JHEP* **12** (2019) 149, [arXiv:1909.07894 \[hep-ph\]](#).
- [102] I. Baldes, Y. Gouttenoire, F. Sala, and G. Servant, “Supercool composite Dark Matter beyond 100 TeV,” *JHEP* **07** (2022) 084, [arXiv:2110.13926 \[hep-ph\]](#).
- [103] A. Azatov and M. Vanvlasselaer, “Phase transitions in perturbative walking dynamics,” *JHEP* **09** (2020) 085, [arXiv:2003.10265 \[hep-ph\]](#).
- [104] W.-Y. Ai, J. S. Cruz, B. Garbrecht, and C. Tamarit, “Instability of bubble expansion at zero temperature,” *Phys. Rev. D* **107** no. 3, (2023) 036014, [arXiv:2209.00639 \[hep-th\]](#).
- [105] J. R. Espinosa, T. Konstandin, J. M. No, and G. Servant, “Energy Budget of Cosmological First-order Phase Transitions,” *JCAP* **06** (2010) 028, [arXiv:1004.4187 \[hep-ph\]](#).
- [106] M. Laine, “Bubble growth as a detonation,” *Phys. Rev. D* **49** (1994) 3847–3853, [arXiv:hep-ph/9309242](#).
- [107] T. Krajewski, M. Lewicki, and M. Zych, “Hydrodynamical constraints on the bubble wall velocity,” *Phys. Rev. D* **108** no. 10, (2023) 103523, [arXiv:2303.18216 \[astro-ph.CO\]](#).
- [108] L. Leitaο and A. Megevand, “Hydrodynamics of phase transition fronts and the speed of sound in the plasma,” *Nucl. Phys. B* **891** (2015) 159–199, [arXiv:1410.3875 \[hep-ph\]](#).
- [109] F. Giese, T. Konstandin, and J. van de Vis, “Model-independent energy budget of cosmological first-order phase transitions—A sound argument to go beyond the bag model,” *JCAP* **07** no. 07, (2020) 057, [arXiv:2004.06995 \[astro-ph.CO\]](#).
- [110] F. Giese, T. Konstandin, K. Schmitz, and J. van de Vis, “Model-independent energy budget for LISA,” *JCAP* **01** (2021) 072, [arXiv:2010.09744 \[astro-ph.CO\]](#).
- [111] J. Ellis, M. Lewicki, and J. M. No, “On the Maximal Strength of a First-Order Electroweak Phase Transition and its Gravitational Wave Signal,” *JCAP* **04** (2019) 003, [arXiv:1809.08242 \[hep-ph\]](#).
- [112] M. Fairbairn, E. Hardy, and A. Wickens, “Hearing without seeing: gravitational waves from hot and cold hidden sectors,” *JHEP* **07** (2019) 044, [arXiv:1901.11038 \[hep-ph\]](#).
- [113] A. Kurkela and G. D. Moore, “Thermalization in Weakly Coupled Nonabelian Plasmas,” *JHEP* **12** (2011) 044, [arXiv:1107.5050 \[hep-ph\]](#).
- [114] W.-Y. Ai, R. Jinno, X. Nagels, and M. Vanvlasselaer, “Dynamical evolution of bubble walls and hydrodynamics.” *in preparation*.
- [115] R. Jinno, T. Konstandin, H. Rubira, and I. Stomberg, “Higgsless simulations of cosmological phase transitions and gravitational waves,” *JCAP* **02** (2023) 011, [arXiv:2209.04369 \[astro-ph.CO\]](#).